

Ⓞ Examination of the Physical Atmosphere in the Great Lakes Region and Its Potential Impact on Air Quality—Overwater Stability and Satellite Assimilation

RICHARD T. MCNIDER,^a ARASTOO POUR-BIAZAR,^b KEVIN DOTY,^b ANDREW WHITE,^a YULING WU,^b MOMEI QIN,^c YONGTAO HU,^c TALAT ODMAN,^c PATRICIA CLEARY,^d ELADIO KNIPPING,^e BRIGHT DORNBLASER,^f PIUS LEE,^g CHRISTOPHER HAIN,^h AND STUART MCKEENⁱ

^a *Department of Atmospheric Science, University of Alabama in Huntsville, Huntsville, Alabama*

^b *Earth System Science Center, University of Alabama in Huntsville, Huntsville, Alabama*

^c *School of Civil and Environmental Engineering, Georgia Institute of Technology, Atlanta, Georgia*

^d *Department of Chemistry, University of Wisconsin–Eau Claire, Eau Claire, Wisconsin*

^e *Electric Power Research Institute, Washington, D.C.*

^f *Texas Commission on Environmental Quality, Austin, Texas*

^g *NOAA Air Resources Laboratory, Silver Spring, Maryland*

^h *NASA Short-Term Prediction Research and Transition Center, Huntsville, Alabama*

ⁱ *NOAA Aeronomy Laboratory, Boulder, Colorado*

(Manuscript received 19 December 2017, in final form 9 August 2018)

ABSTRACT

High mixing ratios of ozone along the shores of Lake Michigan have been a recurring theme over the last 40 years. Models continue to have difficulty in replicating ozone behavior in the region. Although emissions and chemistry may play a role in model performance, the complex meteorological setting of the relatively cold lake in the summer ozone season and the ability of the physical model to replicate this environment may contribute to air quality modeling errors. In this paper, several aspects of the physical atmosphere that may affect air quality, along with potential paths to improve the physical simulations, are broadly examined. The first topic is the consistent overwater overprediction of ozone. Although overwater measurements are scarce, special boat and ferry ozone measurements over the last 15 years have indicated consistent overprediction by models. The roles of model mixing and lake surface temperatures are examined in terms of changing stability over the lake. From an analysis of a 2009 case, it is tentatively concluded that excessive mixing in the meteorological model may lead to an underestimate of mixing in offline chemical models when different boundary layer mixing schemes are used. This is because the stable boundary layer shear, which is removed by mixing in the meteorological model, can no longer produce mixing when mixing is rediagnosed in the offline chemistry model. Second, air temperature has an important role in directly affecting chemistry and emissions. Land–water temperature contrasts are critical to lake and land breezes, which have an impact on mixing and transport. Here, satellite-derived skin temperatures are employed as a path to improve model temperature performance. It is concluded that land surface schemes that adjust moisture based on surface energetics are important in reducing temperature errors.

1. Introduction

High mixing ratios of ozone along the shores of Lake Michigan have been a major problem for air quality agencies in the region for nearly 40 years (Lyons and Cole 1976; Foley et al. 2011). Exceedances of both the

older 1-h ozone regulatory standard and the newer 8-h standard have occurred in the four-state area (Illinois, Indiana, Michigan, and Wisconsin). Although the number of ozone events and severity of exceedances have decreased over the last 20 years, violations still continue in the region, especially along the western shore of Lake Michigan (Cleary et al. 2015). It is important to understand the influence of Lake Michigan on local meteorology and its role in past air quality issues. Keen and Lyons (1978) described the characteristics of the Lake Michigan sea breeze in light of traditional conceptual models of lake-breeze systems, with an emphasis

Ⓞ Denotes content that is immediately available upon publication as open access.

Corresponding author: Arastoo Pour-Biazar, biazar@nsstc.uah.edu

DOI: 10.1175/JAMC-D-17-0355.1

© 2018 American Meteorological Society. For information regarding reuse of this content and general copyright information, consult the [AMS Copyright Policy \(www.ametsoc.org/PUBSReuseLicenses\)](https://www.ametsoc.org/PUBSReuseLicenses).

on the onshore convergence lines that can transport pollutants aloft into the offshore return circulation. [Levy et al. \(2010\)](#) provided a comprehensive list of the physical related factors that affect local lake- and land-breeze circulations such as shoreline curvature, urban land use, and synoptic settings. [Lyons and Cole \(1976\)](#) discussed the impact of the thermal destruction of the lake-breeze flow as it moves inland producing local high concentrations as well as the long-range effects of combined recirculation and alongshore transport of urban and power plant plumes.

Overwater, offshore ozone production has also been cited as a mechanism for high ozone concentrations in coastal areas. After being intimated in early conceptual models of the Lake Michigan lake-breeze systems ([Lyons and Cole 1976](#)), aircraft measurements ([Dye et al. 1995](#); [Foley et al. 2011](#)) have verified high mixing ratios of ozone aloft over the lake. [Dye et al. \(1995\)](#) characterized the lake breeze as a near perfect reaction chamber with precursors imported from the urban areas, large photolysis rates resulting from clear skies in the subsidence zones over the lake, and a lack of surface losses from deposition or nitrogen oxides (NO_x) titration. The high ozone concentrations in this reaction chamber can then be brought back to shore, although often translated alongshore, creating high coastal ozone mixing ratios.

More recent papers in the literature, supported by new observations and modeling, have also discussed the role of overwater stability in affecting ozone concentrations. [Goldberg et al. \(2014\)](#) noted for the Chesapeake Bay that higher overwater ozone concentrations are supported by 1) shallower boundary layers trapping shipping emissions near the surface, 2) higher photolysis rates resulting from clear skies over the bay, 3) decreased boundary layer venting as a result of a lack of fair-weather cumulus clouds, and 4) slower deposition losses over water. [Loughner et al. \(2014\)](#) also discussed the important role of model resolution in capturing elements of the overwater ozone behavior. For Chesapeake Bay, a 1.33-km horizontal mesh was needed to capture the structure.

A recurring theme in the Great Lakes region has been the role of the land-lake breeze in transporting and diluting precursors ([Dye et al. 1995](#)). [Banta et al. \(2005\)](#) more recently provided an excellent review of how the sea breeze in the Houston, Texas, area influences precursor concentrations and the transport and recirculation of the precursors and ultimately ozone. [Banta et al. \(2011\)](#) provided a discussion of the role that meteorological conditions play in a coastal setting. Of particular importance are the developments of stagnant zones over emission regions as the thermal circulation balances the synoptic forcing.

The shared problem of high coastal ozone concentrations for states in the Great Lakes region has led to cooperation among state air quality agencies ([LADCO 1995](#)). This cooperation has spurred a series of intensive observational field programs and modeling studies that have attracted national scientific resources to the Lake Michigan air quality problem—most recently the 2017 Lake Michigan Ozone Study (LMOS 2017; see [Pierce et al. 2017](#)).

Several physical issues are addressed in this paper:

- 1) The first is overprediction of surface ozone over water by models for Lake Michigan. [Fast and Heilman \(2003\)](#) and [Cleary et al. \(2015\)](#) show that overprediction of surface ozone over water as based on ferry data seems to be a consistent feature in model performance. Here the role of mixing having an impact on overwater atmospheric stability is examined in meteorological models, and the effect of mixing on surface ozone is tested in air quality sensitivity simulations.
- 2) Another is improvement in model prediction of temperature in the Great Lakes region. Temperature plays a major role in emissions and chemical kinetics, especially thermal decomposition of nitrogen species. In addition, as noted by [Levy et al. \(2010\)](#), land-water temperature contrasts play a pivotal role in controlling the strength and timing of the lake- and land-breeze and mixing processes. New techniques using satellite datasets are examined for improving temperature predictions.

The studies below examine meteorological performance for a longer time scale (at least one month of simulation) for 2009, 2011, 2012, and 2013. These years cross a variety of conditions from a relatively moist and cool 2011 to an extraordinarily hot and dry 2012. Thus, we do not emphasize the complex details of individual lake-breeze or high-ozone events.

2. Overwater overprediction of surface ozone

Early studies of Lake Michigan meteorological behavior ([Lyons and Cole 1976](#)) discussed the role of cold lake surface temperatures as the cause of high ozone mixing ratios over the lake. With the advent of aircraft observations ([Dye et al. 1995](#), [Foley et al. 2011](#)), very high amounts of precursors and ozone were found aloft over the lake. The origins of these high concentrations are described by [Dye et al. \(1995\)](#), who pictured a meteorological system in which land-based emissions are transported offshore, either as part of the offshore land breeze at night or the return branch of the lake-breeze circulation during the day. [Figure 1](#) shows a schematic of

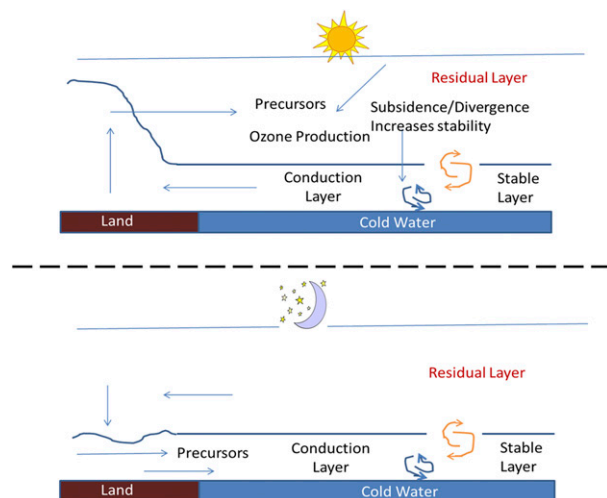


FIG. 1. Schematic of Lake Michigan lake-breeze systems after Foley et al. (2011) and Adamski (2003). (top) The daytime lake-breeze circulation; (bottom) the nighttime/early-morning land breeze.

these processes adapted from Foley et al. (2011) and Adamski (2003), with additional notations on turbulent mixing processes. Dye et al. (1995) referred to the stable layer over the lake as a conduction layer, indicating that turbulence levels are small. Aircraft observations confirmed the high amounts of ozone offshore in the conduction layer over the lake just as postulated in the Dye et al. (1995) schematic. Ozone mixing ratios aloft over the western part of the lake in two cases [at 1430 central daylight time (CDT) 18 July 1991 and 1400 CDT 26 June 1991] showed maximum levels of 180 ppb at the 125- to 130-m layer above the surface.

Modeling studies have indicated that surface ozone over the lake is overpredicted relative to ship measurements of surface ozone. Fast and Heilman (2003) using the coupled meteorological–chemical Pacific Northwest National Laboratory (PNNL) Eulerian Gas and Aerosol Scalable Unified System model (PEGASUS), compared modeled ozone with ferry observations along the ferry path from Manitowoc, Wisconsin, to Ludington, Michigan, between 15 July and 14 August 1999. Their scatterplot showed that the model largely overpredicted ozone relative to the surface ferry measurements.

Cleary et al. (2015) more recently compared surface ozone predictions from NOAA’s National Air Quality Forecast System using the Community Multiscale Air Quality (CMAQ) model (Janjić 2003; Eder et al. 2009; Byun and Schere 2006) with ferry observations along the ferry path from Milwaukee, Wisconsin, to Muskegon, Michigan, during the summer of 2009. Cleary et al. (2015) demonstrated consistent overprediction by the model across the summer ozone season. Their study indicated

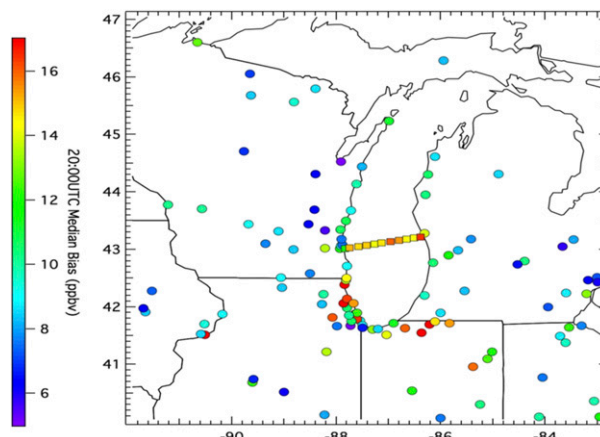


FIG. 2. Spatial plot of NOAA CMAQ bias in the Lake Michigan region, showing consistent overprediction along the ferry plot [from Cleary et al. (2015)] relative to land sites. The CMAQ model ozone bias for EPA station air quality monitors is shown with circles, and for the *Lake Express* ferry with squares. EPA monitor biases are calculated at 2000 UTC (1500 CDT), and the data have been winnowed for only those days for which ferry data are available. The ferry data are from the 1230–1500 CDT transect statistics.

that the maximum observed ozone occurred in the mid-afternoon, and that was also the time of largest model overprediction. The CMAQ model analyzed by Cleary et al. (2015) showed that overwater surface overprediction was consistently greater than overland sites (Fig. 2), although there were sites in northern Indiana that were also overpredicted.

Because the consistent overprediction in Fast and Heilman (2003) and Cleary et al. (2015) occurs in the stable atmosphere over the lake, in this investigation we examine the model simulation of the stable atmosphere and its possible role in the model overprediction. This is not to rule out that emission errors and/or chemical mechanisms might be responsible for the model discrepancies over water, but here we investigate whether boundary layer formulations and their impact on stability may have a role in model overprediction. Goldberg et al. 2014 discussed the role of physical factors including stability increasing ozone concentrations over Chesapeake Bay. Loughner et al. (2014) showed that CMAQ overpredicted surface ozone over Chesapeake Bay relative to ship observations, but the overwater overestimate in CMAQ in these episodic studies was not greater than for land stations. Also, lake surface water temperatures can have an impact on near surface stability and mixing (Fast and Heilman 2003).

a. Background on stable boundary layer mixing

Because of cool lake temperatures, the lower atmosphere over the Great Lakes is generally stable during the warm ozone season. Bosveld et al. (2014) in an intermodel

comparison study showed much greater spread in the model stable-layer performance than in convective conditions, which leads to concern about uncertainties in modeling the stable boundary layer behavior over the lake. In the 1980s, models began using local mixing schemes (e.g., Blackadar 1979; Mellor and Yamada 1982) for the stable boundary layer and employing turbulent kinetic energy models or stability function closures based on Monin–Obukov similarity functions (Businger 1973). As a result, models began to have a problem of becoming too stable, with surface conditions becoming too cold and calm. Mixing of heat and momentum (or ozone) to the surface was too strongly suppressed (Beljaars and Holtslag 1991; McNider et al. 2012). In these coarse grid models, it appeared that additional mixing was needed (Savijärvi 2009). This was often implemented by using longer-tailed stability functions in turbulent mixing schemes. In K closure models in the stable boundary, the vertical mixing is often parameterized (Blackadar 1979; Savijärvi 2009) by

$$K = f(\text{Ri})l^2s, \quad (1)$$

where Ri is the local gradient Richardson number, l is a mixing length, and s is the local shear. Figure 3 shows the stability functions used or discussed in the present paper. The longer-tailed functions are those that maintain mixing beyond a critical Ri (bulk or gradient) of about 0.25. The England–McNider and the Pleim polynomial stability functions would be short-tailed forms, whereas the Beljaars–Holtslag and Louis stability functions would be considered longer-tailed forms (these functions are discussed in more detail below). With this as background, Savijärvi (2009) summarizes the issue very well: operational models often had too much mixing, resulting in temperature and wind overprediction, especially over oceans and homogeneous settings.

Further, in the 15–20 years since the inadequate mixing began to be addressed (by adding mixing), it appears that, with increased vertical resolution and/or improved radiation schemes, models were making the opposite error, now having too much mixing (Steenefeld et al. 2008; McNider et al. 2012; Savijärvi 2009). This then led to an environment in the model that was too warm and windy at the surface. This was also seen in air pollution studies (Garcia-Menendez et al. 2013; Ngan et al. 2013; Lee et al. 2014) with too much downward mixing of heat, momentum, and ozone from aloft at night. The modifications to models to increase mixing discussed above went beyond adjusting stability functions. Other adjustments such as making the critical Richardson number (bulk or gradient) a function of grid spacing (McNider and Pielke 1981), setting minimum values for vertical eddy diffusivities, or setting minimum values of

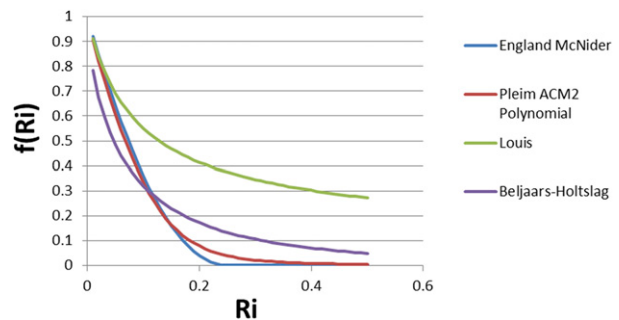


FIG. 3. Stability function $f(\text{Ri})$ forms used or mentioned in this investigation [England–McNider: England and McNider (1995); Pleim ACM2 polynomial: Pleim (2007); Beljaars–Holtslag: Beljaars and Holtslag (1991); Louis: Louis (1979) and Poulos et al. (2002)].

surface friction velocity were employed. On the basis of these historical trends in meteorological models, the hypothesis tested in this paper is that enhanced mixing in the meteorological model was partly responsible for the overwater overprediction seen in CMAQ by Cleary et al. (2015).

b. WRF modeling of the 2009 case

Before addressing and testing the “too much mixing hypothesis,” it is felt that a basic understanding of the current Weather Research and Forecasting (WRF) Model performance for 2009 and sensitivity to different mixing and land surface schemes is needed. The WRF Model with the Advanced Research core (WRF-ARW; see Skamarock et al. 2008) at a horizontal resolution of 12 km was employed to model the meteorological conditions of a significant portion of the 2009 ozone season (1 July–4 September 2009) as reported by Cleary et al. (2015). The WRF-ARW, version 3.8.1, was employed in the current study. Note that the operational CMAQ for the 2009 period employed meteorological fields provided by the operational North American Model (NAM-12), which was the NCEP version of the WRF Model (WRF-NMM) with a horizontal resolution of 12 km. The 2009 CMAQ and NAM-12 versions are also not identical to the current CMAQ and NAM-12, which have undergone improvements, including updated emission inventories for CMAQ (Lee et al. 2017).

In the Lake Michigan area there have been special observation programs. However, individual events can sometimes be difficult to replicate, given large changes in the lake-breeze system that can occur because of uncertainty in initial and boundary conditions. The Cleary et al. (2015) results are remarkable in their consistency over a 2.5-month period. Here we follow the strategy of Fast and Heilman (2003) of running the model over a

TABLE 1. WRF configuration for the Control simulation.

Category	Selection
Time step	30 s
Grid spacing	12-km horizontal; 41 layers up to 50 hPa
Microphysics	Morrison 2-moment ^a
Longwave/ shortwave radiation	RRTMG ^b
Radiation update frequency	10 min
Surface layer	Pleim–Xiu ^c
Land surface model	Pleim–Xiu ^d
PBL	ACM2 ^e
Cumulus parameterization	Kain–Fritsch ^f with moisture-advection- modulated trigger function ^g
Nudging	No nudging in PBL or below 2 km
Pleim surface nudging	0 (turned “off”)
Nudging coefficients	10^{-4} for wind and temperature; 10^{-5} for water vapor
Land-use dataset	USGS for 2009 and NLCD for 2012 and 2013 simulations

^a Morrison et al. (2009).

^b Iacono et al. (2008).

^c Pleim (2006).

^d Pleim and Xiu (1995).

^e Pleim (2007).

^f Kain (2004).

^g Ma and Tan (2009).

long period to examine mean model behavior. It is assumed that such understanding will apply to modeling extreme events.

c. Baseline model evaluation

The WRF Model setup and physics choices are given in Table 1 (hereinafter the baseline is referred to as Control). The continental domain with a 12-km resolution and subdomains for statistics given below are shown in Fig. 4. The Asymmetric Convective Model, version 2 (ACM2), PBL (Pleim 2007) was chosen because it is the PBL scheme used in CMAQ. The Pleim–Xiu land surface model (Pleim and Xiu 1995) was also chosen because of consistency with Pleim (2007) and because of the data assimilation of surface moisture and deep soil temperature (Pleim and Xiu 2003; Pleim and Gilliam 2009) using surface observations (described more in section 3). These have been widely used in air quality studies and represent one of the few PBL and land surface schemes developed from an air quality perspective. Hereinafter, the Pleim (2007) PBL will be referred to as ACM2 and the land surface model will be called P–X.

The WRF physics options employed in the simulation include the Rapid Radiative Transfer Model for General Circulation Models (RRTMG) radiation



FIG. 4. Schematic of approximate model domains used in the studies (red boxes) and subdomains for statistical evaluation (blue outlines). The outer blue line around the lake represents the 20–100-km statistical domain, and the inner line represents the <20-km statistical domain. The area between the outer blue line and the red box represents the >100-km domain as used in Figs. 5 and 6. The outer red box is the WRF 12-km domain.

scheme (Iacono et al. 2008), 2-moment Morrison microphysics scheme (Morrison and Gettelman 2008), and Kain–Fritsch convective scheme (Kain 2004) with the moisture-advection-based trigger (Ma and Tan 2009). The National Land Cover Database 2011 (NLCD-2011) was used as the land-use/land-cover data in the 2012 and 2013 simulations.

The WRF Model was run from 1 July to 4 September 2009 using 5.5-day segments reinitializing from the NAM-12 analyses with a 12-h spinup. During the 5-day segment, nudging to the NAM-12 analysis fields was carried out above 2 km. To be consistent with the 2009 NAM/CMAQ simulation used in Cleary et al. (2015), the P–X observed moisture nudging and deep temperature were not used in the Control simulation. Initial soil moisture was provided via the NAM analysis in that the soil moisture was reinitialized for each 5-day segment in the model period. The data assimilation of moisture from the NOAA/NCEP–Oregon State University–Air Force Research Laboratory–NOAA/Office of Hydrology (“Noah”) land surface/land data assimilation system was included via this process. Figure 5 shows the basic model performance statistics for the 2-m temperature and 10-m wind speed for the Control case for overland sites in 2009. The model evaluation statistics over land were based on the “METSTAT” statistical package developed by Ramboll Environ, Inc., (<http://www.camx.com/download/support-software.aspx>). Figure 5 also includes statistics from other simulations that were performed to investigate the impact of land surface and PBL choices on the results. The abbreviations and the key model changes for each simulation are listed in Table 2.

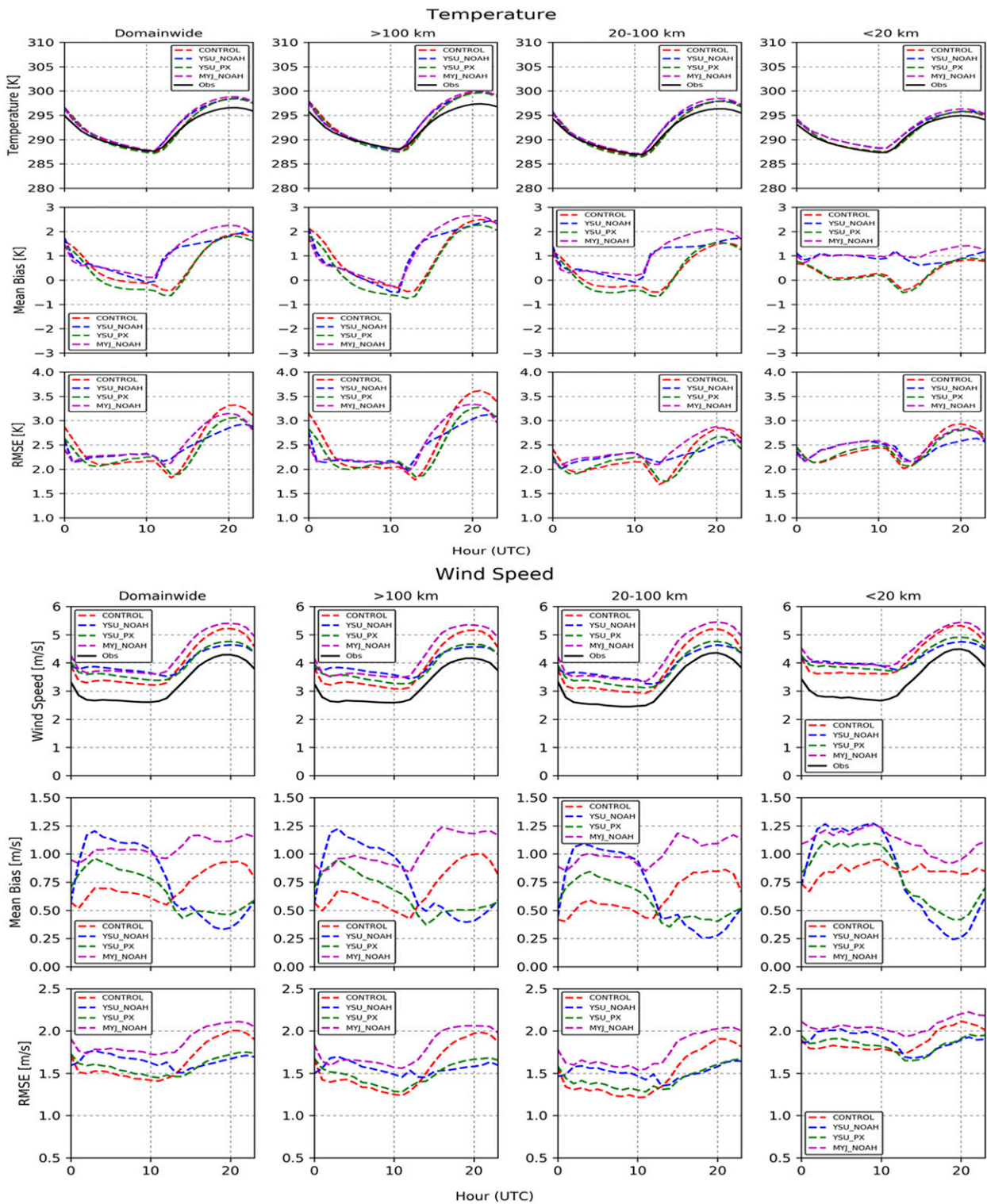


FIG. 5. Model evaluation statistics for 2-m (top) temperature and (bottom) wind speed on the full domain and subdomains in the Great Lakes region for the period from 1 Jul 2009 through 4 Sep 2009. The areas encompassing the statistical domains are given in Fig. 4. Statistics are given for the base Control case (with P-X PBL and surface scheme), the YSU PBL with P-X surface scheme, YSU PBL with Noah surface scheme, and the MYJ PBL with Noah surface scheme.

TABLE 2. Run abbreviation categories.

Run abbreviation	GOES insolation	MODIS-derived greenness	Soil moisture nudging	Heat capacity adjustment	PBL scheme	LSM scheme	Changes to Pleim PBL scheme	MODIS skin_T for Great Lakes	Years
Control	No	No	No	No	ACM2	P-X	No	No	2009; 2012; 2013
INSL	Yes	No	No	No	ACM2	P-X	No	No	2012; 2013
VEG	Yes	Yes	No	No	ACM2	P-X	No	No	2013
SM	Yes	Yes	Yes	No	ACM2	P-X	No	No	2013
HC	Yes	Yes	Yes	Yes	ACM2	P-X	No	No	2013
PBL	No	No	No	No	ACM2	P-X	Yes	No	2009
MODIS	No	No	No	No	ACM2	P-X	Yes	Yes	2009
YSU-Noah	No	No	No	No	YSU	Noah	No	No	2009
YSU-P-X	No	No	No	No	YSU	P-X	No	No	2009
MYJ-Noah	No	No	No	No	MYJ	Noah	No	No	2009

In addition to the Control simulation, WRF simulations for several land surface and PBL schemes were performed to examine the sensitivity of overwater profiles to boundary layer and surface parameterizations, especially in regards to relative amounts of vertical mixing. Later, a sensitivity run of the CMAQ model for large and small mixing cases was carried out to see the impact on overwater ozone. For the base Control case, the 2-m temperature performance (Fig. 5 top) is reasonable with an average bias (model minus observed) of less than 1°C. The reduced diurnal temperature range is seen in the 20-km domain closest to the lake. The largest negative bias (cool bias) occurs in the overnight, whereas positive bias occurs in the afternoon. The slight cool bias at night may not be consistent with our hypothesis that the model is not stable enough. The largest root-mean-square error (RMSE) occurs in the afternoon, perhaps representing issues with prescribing land-use parameters in the surface scheme.

Here we provide sensitivity studies for several PBL schemes used within the air quality community. Previously, Hu et al. (2013) provided a comparison of the Pleim (2007) scheme (ACM2), the Mellor–Yamada–Janjić (MYJ) scheme (Janjić 2003), and the Yonsei University (YSU) scheme (Hong et al. 2006) for a Texas field program. In the Hu et al. (2013) study, all of the PBL schemes were coupled to the Noah land surface scheme (Ek et al. 2003).

While the Pleim ACM2 scheme is used in CMAQ, the NAM model that drove CMAQ in 2009 employs the MYJ scheme (Siuta et al. 2017). In NAM, the MYJ scheme is coupled with the Noah land surface scheme. Figure 5 shows the WRF Model performance for the MYJ scheme coupled with Noah in comparison with the Control simulation. Figure 5 also provides comparisons between the YSU and the Control case. The YSU Noah and MYJ Noah for the full domain have less 2-m temperature bias at night in the stable boundary layer but have greater warm bias in the daytime. The two Noah schemes also have a warm bias closer to the lake. The YSU/Noah and MYJ/Noah schemes seem to have more mixing at night in the full domain than some of the other schemes. For the domain near the lake, they have a substantially larger bias in the early morning. It is interesting that this seems to be related to the land surface scheme rather than the boundary layer scheme since both YSU and MYJ coupled with the P-X surface have smaller error. Thus, this behavior may be tied to the surface fluxes that may be different in the two land-use schemes.

d. Modifications to ACM2 to enhance stability (PBL)

The ACM2 mixing scheme for the stable boundary layer (SBL) can be characterized as one with minimal mixing in the SBL since it employs a short-tailed stability

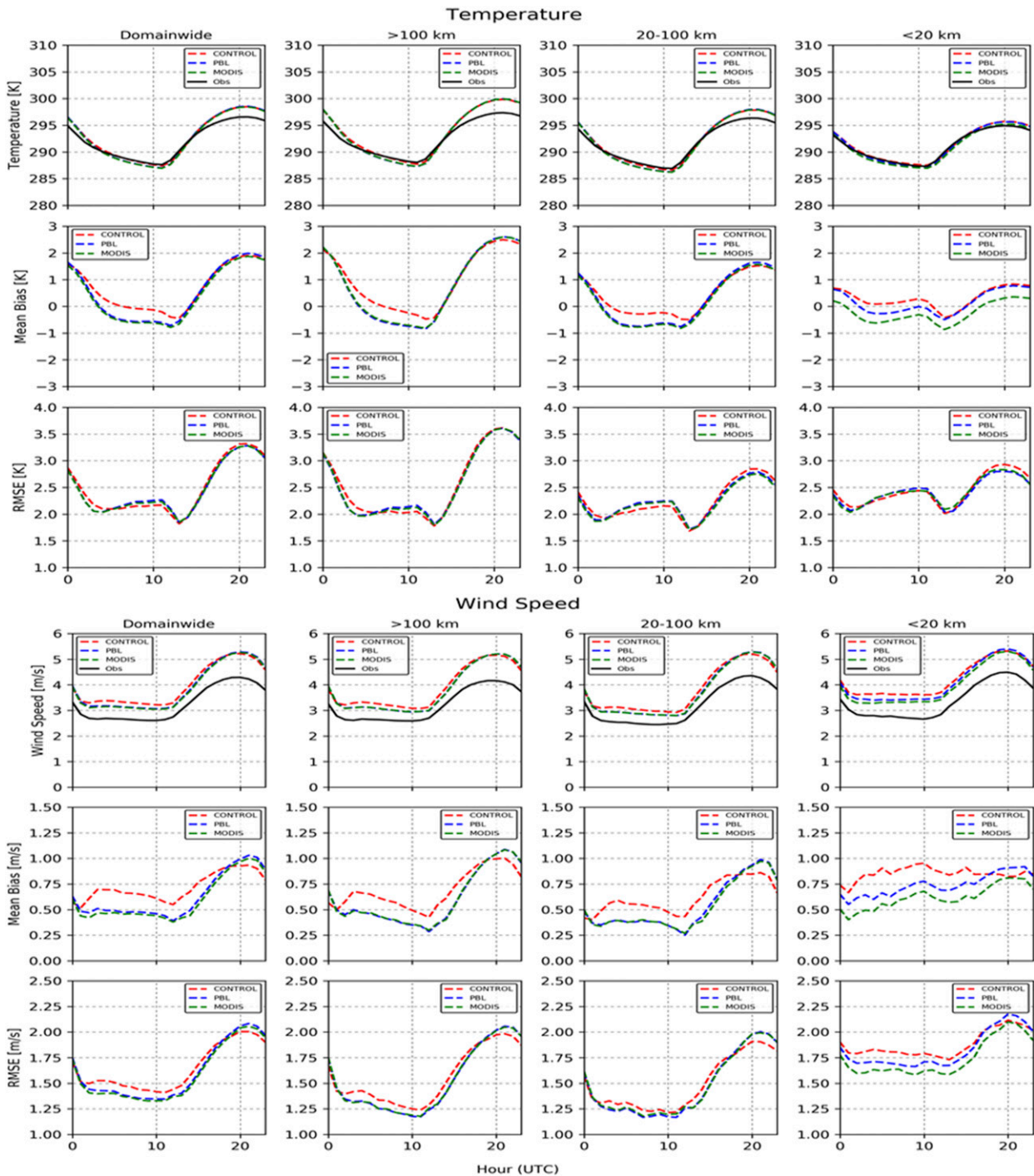


FIG. 6. Model evaluation statistics for 2-m (top) temperature and (bottom) winds on the full and subdomains in the Great Lakes region for the Control (ACM2), PBL (ACM2 modified with enhanced stability), and MODIS (inclusion of MODIS satellite lake surface temperatures).

function. However, as mentioned above, because early coarse-resolution models produced an SBL that was too cool and calm, many PBL schemes added components to increase mixing. The ACM2 had a few of these components, which are discussed in the [appendix](#).

A new model simulation (referred to as PBL) was carried out without these components to produce a scheme with less mixing. [Figure 6](#) provides the impact of these changes on model verification statistics (the impacts of lake surface temperatures discussed below

are also included). As can be seen, the impacts on performance are minor with slightly greater impact near the lake. It does decrease 2-m air temperatures at night indicating a possible increase in stability but the model is still too cool relative to observations. However, when comparing the results from the new modified ACM2 more-stable scheme (PBL) with the Control simulation, significant spatial differences are observed. Figure 7 shows the average differences (New P-X PBL – Control) in surface temperature and wind speed at 2000 UTC over the entire period of simulation for 2009 (from 0000 UTC 1 July 2009 through 1200 UTC 4 September 2009). These differences indicate that the modified ACM2 simulation produces cooler temperatures over the lake leading to stronger sea breezes.

e. Louis scheme

All of the other stable boundary layer schemes discussed and tested above—ACM2 (the control), MYJ, and YSU—can be characterized as short-tail or minimal mixing forms. As mentioned above, it was hypothesized that the meteorology forcing the 2009 CMAQ may have had too much boundary layer mixing in the stable boundary layer over the lake. As will be discussed below, this appears to be supported by the 2009 NAM/CMAQ temperature and wind speed profiles that are substantially less stable and have less shear than the WRF simulations with ACM2, MYJ, YSU, and the modified ACM2 (PBL). To produce a less stable system in WRF that might be comparable to the 2009 NAM/CMAQ simulations another modification was made to the ACM2 scheme in WRF. Rather than using the Pleim polynomial for the stability function that calculates the vertical eddy diffusivity (see Fig. 3), the Louis stability function was employed as in Eq. (A1). Additionally, to ensure consistency the friction velocity and surface fluxes in the P-X surface scheme were calculated using the Louis stability functions for stable conditions (see the appendix). The impacts of the Louis modifications on overwater temperature and wind speed profiles are discussed below. The Louis run is also used as the large mixing case in the CMAQ mixing sensitivity runs below.

f. Role of lake surface temperatures

In addition to PBL mixing schemes, lake surface temperatures can also affect stability. The role of lake temperatures and their seasonal variation has long been an issue in the Great Lakes modeling and in other areas such as the Chesapeake Bay (Appel et al. 2014).

The lake temperatures in CMAQ/NAM for the 2009 simulations were, according to the NCEP online

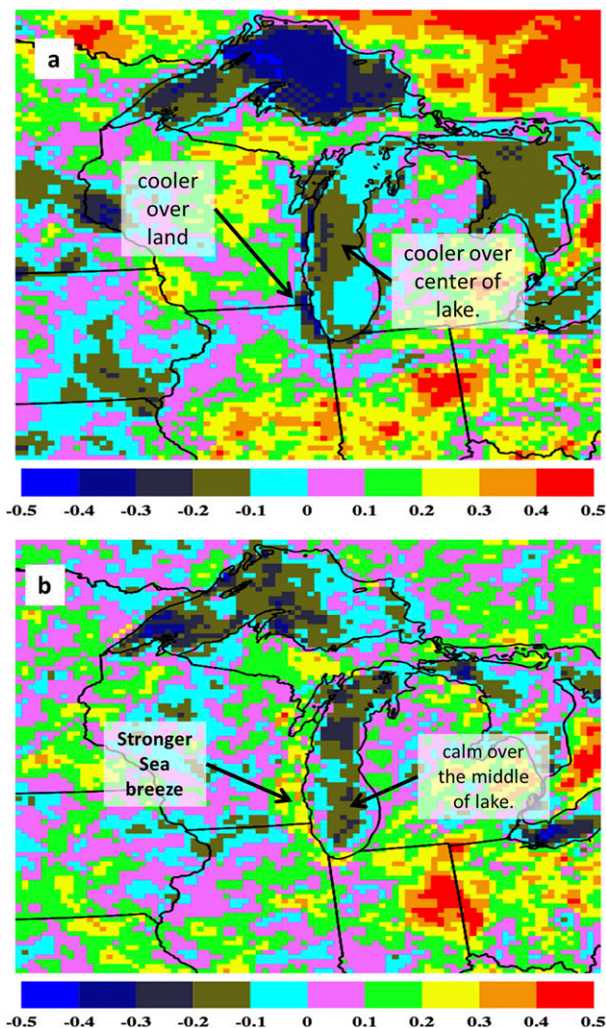


FIG. 7. Average differences in surface (a) temperature and (b) wind speed at 2000 UTC (New P-X PBL – Control). The WRF simulation period was from 0000 UTC 1 Jul 2009 through 1200 UTC 4 Sep 2009.

documentation (<http://www.emc.ncep.noaa.gov/NAM/clog.php>), based on the NOAA–Great Lakes Environmental Research Laboratory (GLERL) SST dataset (<https://www.glerl.noaa.gov/res/glcfs>). The WRF simulations in this study also employed the GLERL lake temperatures that are included as part of the NAM reanalysis. NAM moved to the Real Time Gridded (RTG) SST water temperature (Thiébaux et al. 2003) in 2014 (see http://polar.ncep.noaa.gov/sst/rtg_high_res). Figure 8 shows snapshots of the WRF GLERL lake surface temperatures and MODIS lake surface temperatures and the difference [see Kilpatrick et al. (2015) for background on MODIS SST]. The model GLERL temperatures appear to be consistently warmer than the MODIS lake temperatures. A similar analysis was

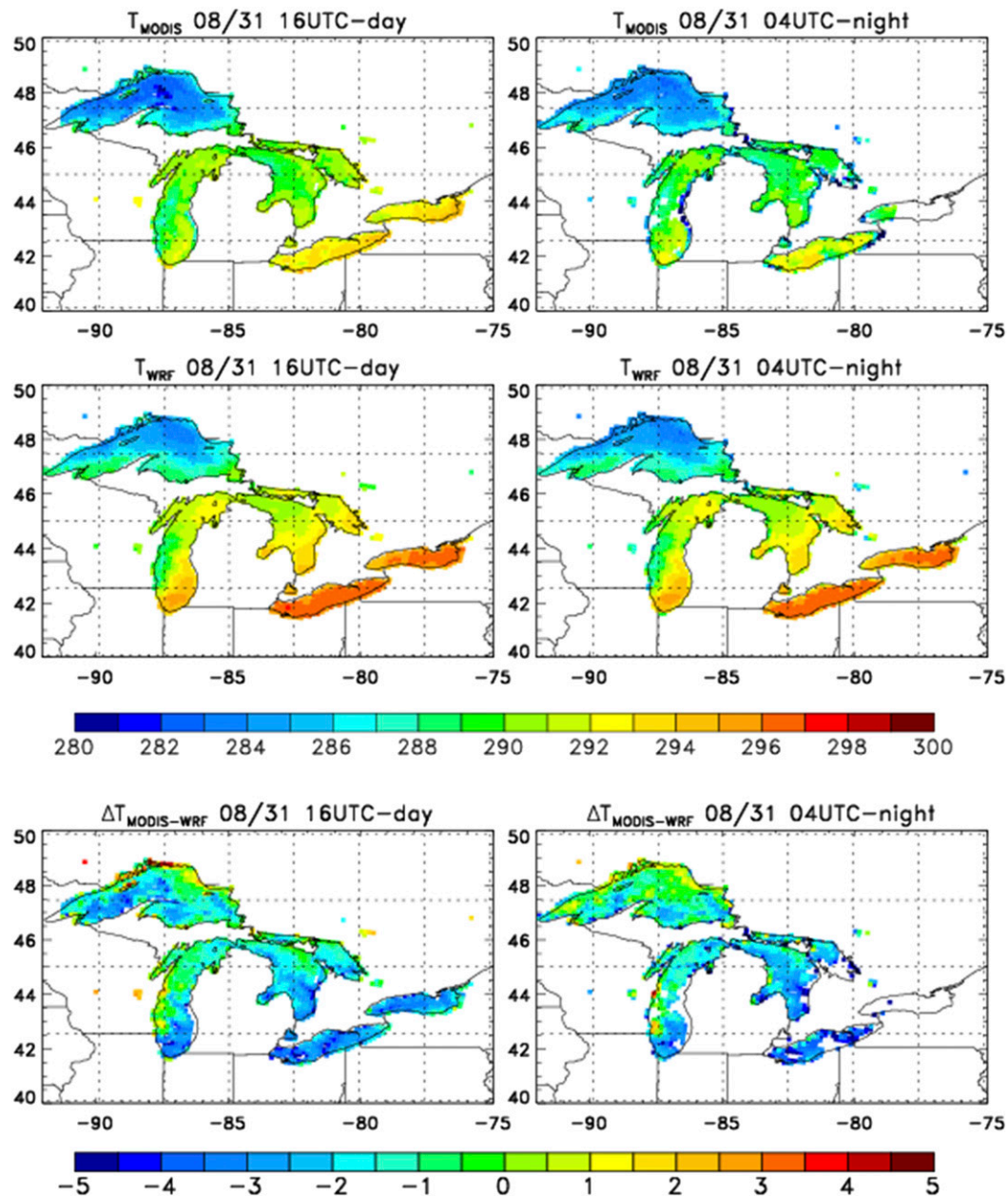


FIG. 8. Snapshots of the WRF GLERL and MODIS lake surface temperatures and their difference at 1600 UTC (daytime) and 0400 UTC (nighttime) 31 Aug 2009.

carried out for 2013 (not shown) that showed similar results of MODIS being cooler than GLERL.

To examine the impact of the lake surface temperatures on WRF simulations a procedure was established to assimilate MODIS SST into WRF through replacement. Because MODIS data often have missing values as a result of clouds, a procedure was established to form a time composite with an 11-day centered running average of the original MODIS SST product. This is consistent with technique proposed by

Knivvel et al. (2010) that used a 12-day running average. Following Knivvel et al. (2010), we also discarded MODIS SST if the 24-h change exceeded 6°C as a means to remove cloud contamination. This daily SST data replaced what WRF had for SST for the Great Lakes only. No time interpolation was done inside WRF, therefore the SSTs were constant over each 1-day period.

Figure 6 provides the impact on ground-level model evaluation statistics due to the insertion of MODIS lake surface temperature (along with the PBL changes

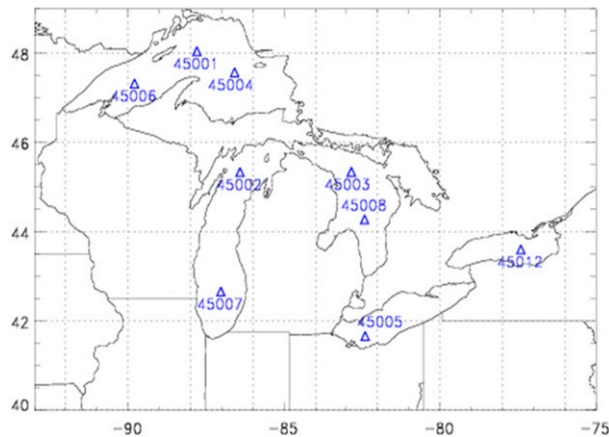


FIG. 9. Map of midlake buoy locations in the Great Lakes, with buoy number.

discussed above). The impact on the model performance was small except for very near the lake.

Since overwater model performance is important, a comparison was made to buoy data over the Great Lakes. Figure 9 provides a depiction of the middle of the lake buoy locations on the Great Lakes. Coastal buoys were not considered. Figure 10 provides time series comparisons for two Lake Michigan buoys for the GLERL and MODIS lake surface temperatures. Buoy water temperature measurement is at approximately 0.6 m deep. The MODIS is a skin temperature and GLERL is a blended temperature. The GLERL is a bit cooler than the buoy temperature, especially for northern Lake Michigan, but the MODIS lake temperature is even cooler. The MODIS low temperature bias seen here could be due to a number of factors (may represent some skin cooling not seen in the GLERL product or possibly a satellite calibration issue as examples) and needs further investigation. Figure 11 provides the model performance statistics relative to buoys for all the Great Lakes and for Lake Michigan alone. Buoy air-temperature measurements are made at 4 m, and wind measurements are at 5 m. The first half-sigma model level (~ 5 m) was used for temperature and wind comparisons. The model air temperatures, both in the Control (label “CNTL”) and the modified PBL (with MODIS SST), are cooler than the buoy for all cases (with MODIS significantly cooler). Note that the model wind speed statistics in comparison to the buoys appear better for the buoys than the land comparisons in Fig. 5. Tables 3 and 4 provide the model temperature and wind statistics against the buoy data. The GLERL temperatures perform much better in the buoy comparisons.

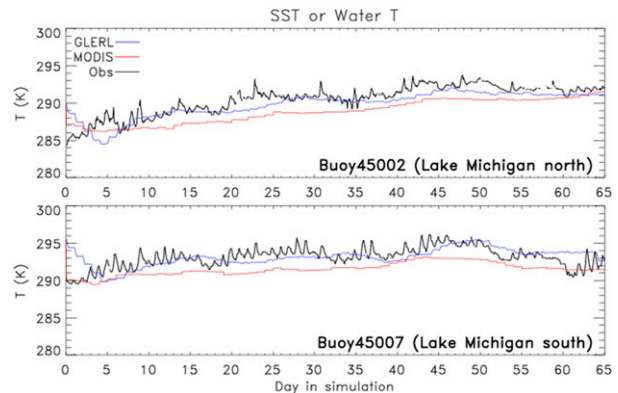


FIG. 10. Time series of SST or water temperature for two Lake Michigan buoys compared with GLERL and MODIS lake temperatures for the simulation period from 1 Jul to 4 Sep 2009. Buoy water temperature measurement is at approximately 0.6 m. The MODIS is a skin temperature (daily), and GLERL is a blended temperature (hourly).

At this point, this preliminary use of MODIS SST should be considered as a sensitivity study. It is not clear that MODIS lake temperatures can be directly used in the current model boundary layer schemes for bottom flux boundary conditions. For example, it may not have the proper corrections to a reference height (see Sun and Mahrt 1995).

g. Overwater wind and temperature profiles

As mentioned above, the main hypothesis in the present investigation is that overwater profiles in NAM/CMAQ were not stable enough resulting in too much vertical mixing. Profiles of temperature and wind were extracted from the WRF Model simulations discussed above for a point over southern Lake Michigan. The profiles for various WRF Model runs and the CMAQ meteorological files used by Cleary et al. (2015) are shown in Fig. 12.

As can be seen in Fig. 12 the profiles of temperature and wind speed from all the current WRF short-tailed forms are relatively similar with the exception of CMAQ and the Louis long-tailed form. It shows that with the additional mixing in Louis, the temperature slope of the Louis case is very close to the 2009 CMAQ profile although there is a temperature offset between the two runs. The average $d\theta/dz$ for the layer from 60 to 500 m above the surface was 7.69, 7.63, and 1.27 K km^{-1} for the NAM/CMAQ, Louis, and Control simulations, respectively. The Louis case wind speed profiles with less shear also agree much better with the 2009 CMAQ profiles. Note that reduced shear not only produces a larger Richardson number but is a direct multiplier in the calculations of mixing coefficients [Eq. (A1)].

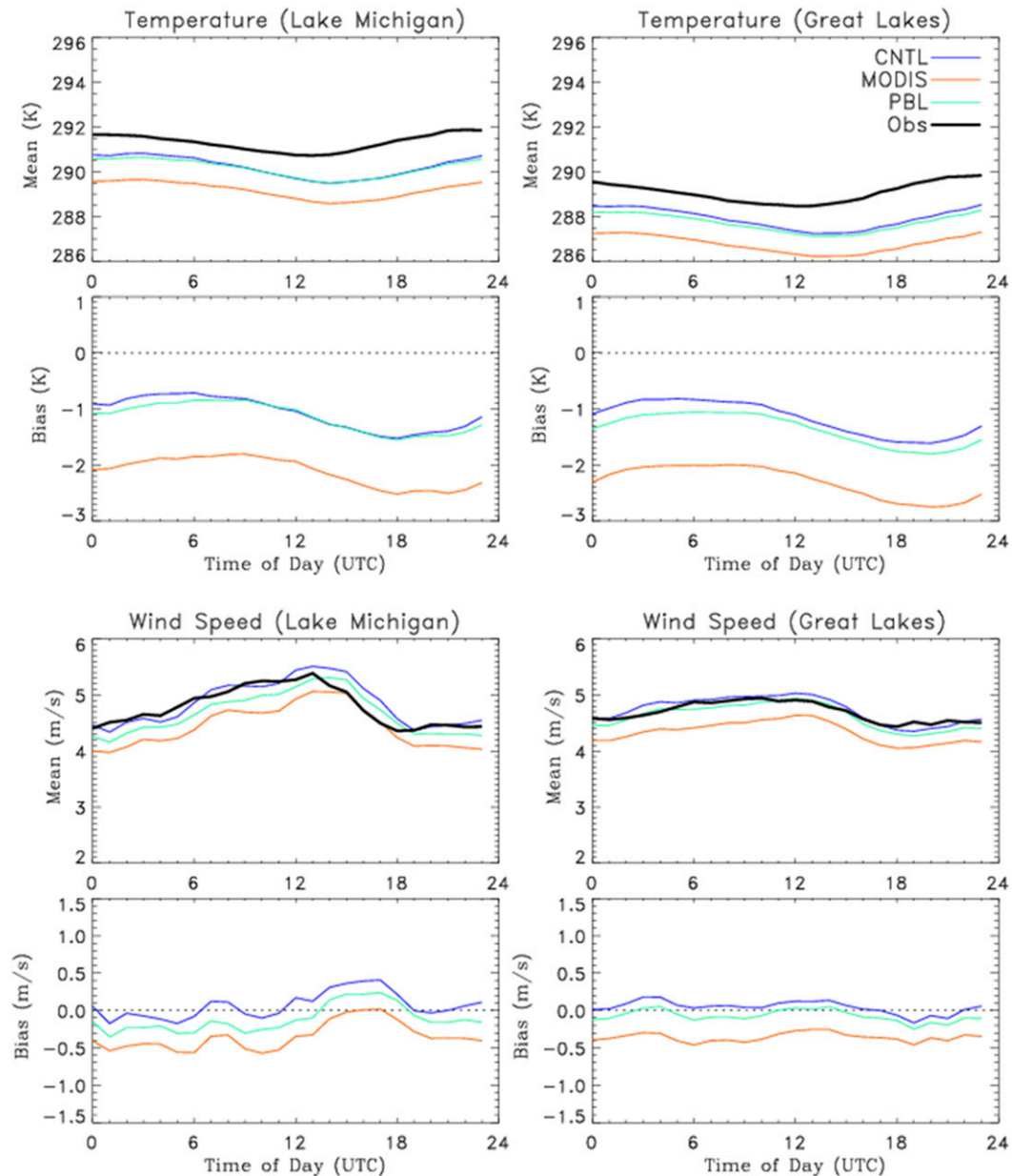


FIG. 11. Model evaluation statistics for air temperature and wind speed from buoy data for (left) Lake Michigan buoys and (right) all Great Lakes buoys for the 2009 simulations. Statistics are based on the entire simulation 1 Jul–4 Sep 2009.

Both of these support the hypothesis that the 2009 NAM driving CMAQ had more mixing than the current WRF runs with short-tailed stability functions.

The comparison of the CMAQ profiles with the current WRF 3.8.1 runs appears to confirm the hypothesis that the CMAQ results in 2009 may be based on temperature and wind speed profiles that were much less stable than the current WRF runs. Note that CMAQ does not directly use the vertical mixing coefficients

from NAM; rather, it diagnoses the mixing coefficients using the ACM2 PBL parameterization. However, the ACM2 scheme in CMAQ uses the temperature and wind speed profiles produced in NAM to calculate local gradient Richardson numbers and bulk Richardson numbers used to diagnose the boundary layer height.

Figure 12 also shows that the MYJ scheme as employed in WRF 3.8.1 here produces one of the most stable profiles. Therefore, there must be a difference in

TABLE 3. Statistics of WRF simulated temperature (K) against buoy measurements for the 2009 simulations.

WRF runs	Lake Michigan			Great Lakes		
	Mean	Bias	RMSE	Mean	Bias	RMSE
Control	290.1	-1.19	2.70	287.8	-1.30	3.29
MODIS	289.2	-2.12	5.65	286.8	-2.30	6.54
PBL	290.2	-1.15	2.69	287.7	-1.36	3.46

TABLE 4. Statistics of WRF simulated wind speed (m s^{-1}) against buoy measurements for the 2009 simulations.

WRF runs	Lake Michigan			Great Lakes		
	Mean	Bias	RMSE	Mean	Bias	RMSE
Control	4.6	-0.20	2.27	4.4	-0.24	2.22
MODIS	4.4	-0.35	3.64	4.3	-0.36	3.34
PBL	4.7	-0.12	3.74	4.6	-0.07	3.32

the MYJ deployed in NAM or there may be adjustments in the friction velocity u_* or minimum diffusivities in NAM as discussed above (as remnants of older strategies to increase mixing in operational models; Savijärvi 2009).

Figure 12 also shows that the adjustments to the ACM2 PBL to reduce mixing (labeled PBL in the figure) did increase stability. The simulation using the MODIS skin temperatures produced the most stable near-surface profile but as noted above produced air temperatures at buoy locations that were too cool. For all the runs using the GLERL lake temperatures, the 1200 UTC plots show an unstable profile near the surface. This may be real or an issue with GLERL temperatures. However, it could be a modeling problem due to inadequate physics related to air–sea interaction in the simulations presented here. Overnight, the model lowest layers will experience clear air radiative cooling. Once the atmosphere cools, however, there is no mechanism for the atmosphere to cool the surface in the current one-way air–sea coupling interactions where the lake temperatures are not dynamically calculated. Evidence of this diurnal change in temperature is seen in the buoy water temperatures that are not included in GLERL or MODIS data (see Fig. 10).

In summary, the current WRF for all of the short-tailed forms produced more-stable profiles (in wind and temperature) than the NAM/CMAQ profile. Thus, it would be assumed that the NAM profiles would have provided greater mixing in CMAQ. However, we show below that this is not necessarily the case. Further, it might be expected that CMAQ run with any of the WRF 3.8.1 boundary layer schemes tested would produce less downward mixing of ozone to the surface than NAM/CMAQ.

A key assumption in our hypothesis that greater mixing would produce higher ozone amounts at the surface is that higher ozone concentrations would exist aloft. The schematic in Fig. 1 shows that over the western lake higher ozone mixing ratios might occur aloft as both biogenic and anthropogenic emissions are carried out over the lake in the return circulation of the lake breeze. Aircraft observations reported in

Dye et al. (1995) for 18 July 1991 showed the observational day-maximum ozone of 180 ppb aloft in the conduction layer (at 125 m), but the two boat observations near the western shore showed maximum ozone of 120–156 ppb.

The Dye et al. (1995) case would support our hypothesis of higher ozone concentrations aloft; however, once we obtained the actual 2009 CMAQ data we could examine model ozone vertical profiles from the model. Using the 2009 CMAQ data, the top of Figs. 13 and 14 show the mean surface ozone and mean surface wind streamlines from the CMAQ model for 1 July–4 September 2009 at 0900 and 1300 local time. Morning surface ozone shows relatively consistent levels of ozone across the domain with some excess scavenging in the urban areas. The morning streamlines show flow from west to east over the domain indicating that, consistent with the Fig. 1 schematic, land-based emissions could be directly transported into the conduction layer over the entire lake. By early afternoon, ozone has increased over the domain. It can be seen that the highest average ozone is over the lake and that in the southern part of the lake the wind regime described by the schematic largely holds, with a lake breeze opposing the mean wind on the western shore and divergence supporting descending motion over the center of the lake. The lower panels of Figs. 13 and 14 show a model east–west vertical cross section near Chicago and at the ferry transect. These show that in the morning the lowest ozone is found at the surface over the lake, especially on the western shore. By early afternoon, the highest ozone is aloft over the western side of the lake but is highest at the surface on the eastern side of the lake. The ozone aloft over the western lake is consistent with the schematic. This vertical distribution is only partially consistent with our hypothesis. Over the western lake, enhanced vertical mixing would perhaps give higher ozone at the surface, but this would not hold over the eastern lake where Cleary et al. (2015) indicated the largest model/ferry discrepancy. It also appears that this surface ozone over the eastern lake is supported by the precursors directly transported into the conduction layer overnight.

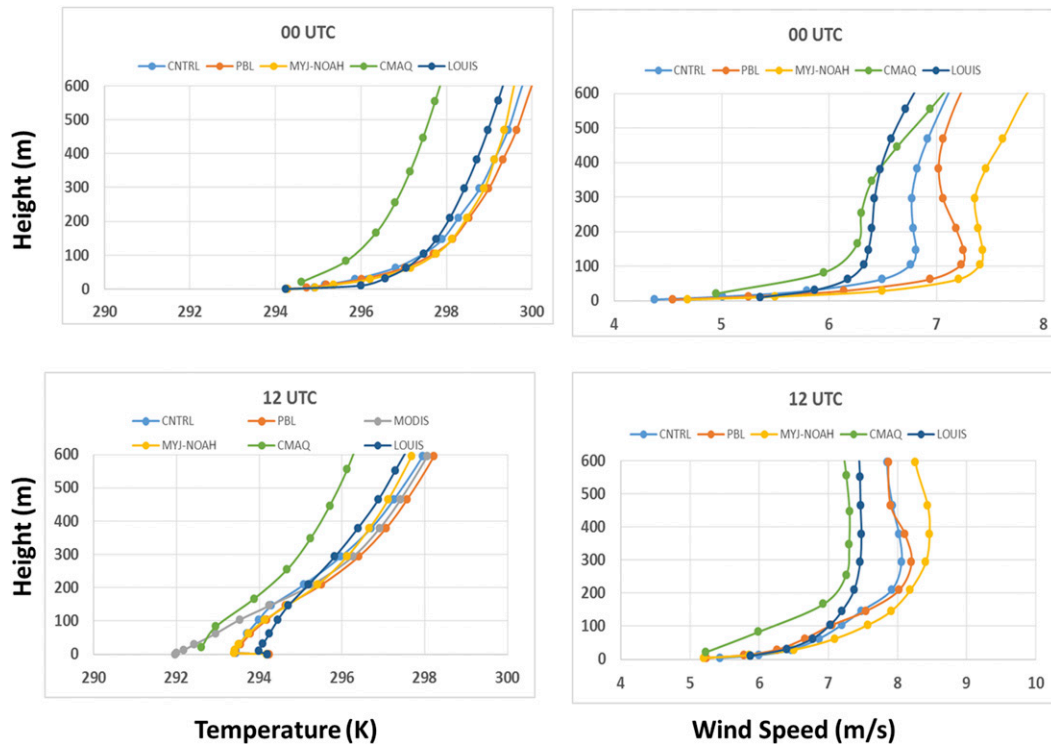


FIG. 12. Potential temperature (K) and wind profiles (m s^{-1}) over Lake Michigan for Control, PBL (modification to ACM2), MYJ-Noah, MODIS, Louis, and CMAQ for the 2009 simulations.

1) CMAQ MIXING SENSITIVITY SIMULATIONS

While the above is not definitive, the evidence of relatively large mixing in the NAM profiles and the combination of maximum ozone and ozone potential being aloft over part of the domain provided an incentive to investigate further. It was recognized that the only proof would lie in making CMAQ sensitivity runs with and without enhanced mixing. It was not possible for our team to reconstruct the emissions for the 2009 case, but we had made July 2011 CMAQ runs for the Great Lakes and had emissions processed. An analysis of the wind field and ozone in the 2011 runs indicated the same general pattern as the 2009 case. Thus, it was decided to carry out the CMAQ sensitivity runs for the month of July 2011. First, a WRF simulation using the ACM2 short-tailed form was made as a control. Next, the simulations were repeated with the Louis adjustments in WRF. Figure 15 shows the WRF Model performance for 2011 for the Control (ACM2) and the Louis form (referred to as Louis). It shows that indeed modifications to increase mixing resulted in increased nocturnal surface winds.

The CMAQ with 2011 emissions was run for the Control and Louis WRF cases. Figure 16 shows the average difference (Louis minus Control) for the month of July in surface ozone between the two runs.

It shows that the case with the additional mixing in WRF increased ozone in CMAQ over Lake Michigan by 8–14 ppb. The patterns and amount of the change were almost identical to the CMAQ 2009 overprediction found by Cleary et al. (2015).

2) INCONSISTENCIES IN DIAGNOSING VERTICAL MIXING IN CMAQ

The evaluation of the CMAQ 2009 wind and temperature profiles showed greater mixing. The CMAQ control versus enhanced-mixing runs showed that surface ozone was increased in the greater mixing case. At this point it might have been considered that the hypothesis of too much vertical mixing in the meteorological model being partly responsible for the 2009 CMAQ-vs-ferry bias was largely confirmed. However, the view of investigators who would argue that too little mixing in CMAQ over water could be partly responsible for model overpredictions was also carefully considered. In looking at the diurnal variation in ozone performance for the Louis and ACM2 cases (see Fig. 17) it was noticed that the Louis case, over land, had smaller surface ozone values overnight than ACM2. This was curious in that normally boundary layer schemes with more mixing bring higher ozone to the surface at night. Thus, it appeared that having the Louis scheme in WRF might have been producing less mixing in CMAQ.

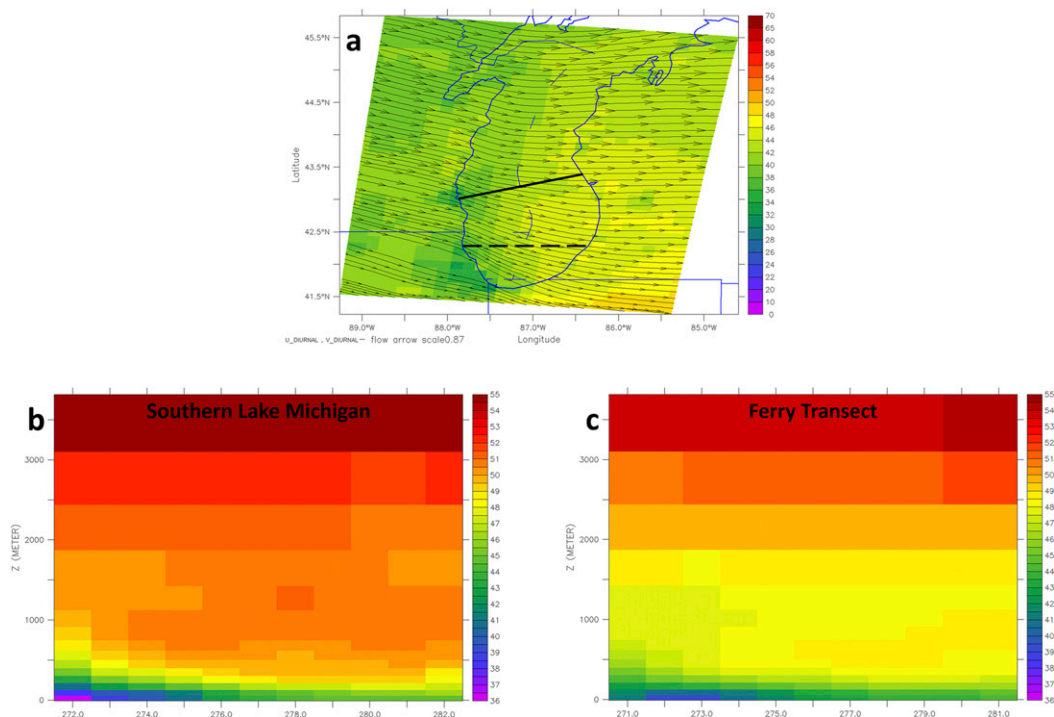


FIG. 13. (a) Average wind field and surface ozone for 1 Jul–4 Sep 2009 from CMAQ 2009 at 0900 local time. The solid line shows the ferry crossing, and the dashed line indicates the southern Lake Michigan traverse. The schematic of Lake Michigan ozone/meteorological conditions in Fig. 1 applies to these cross sections. (b) Average east–west cross section of ozone from CMAQ 2009 model to the south of ferry transect at 0900 local time. (c) Average east–west cross section of ozone from CMAQ 2009 model at ferry transect at 0900 local time.

Thus, another possibility was considered. What if additional mixing in the meteorological model unintentionally produced less mixing in CMAQ?

Vertical eddy diffusivities (hereinafter referred to as K values) in CMAQ are not passed from WRF but are re-diagnosed in CMAQ using the Pleim ACM2 short-tailed form. The K values are re-diagnosed using the wind and temperature profiles from WRF. If vertical gradients of wind speed and temperature have already been smoothed by an enhanced-mixing scheme, then it is possible that the CMAQ diagnosed K s might be less in the enhanced-mixing WRF case than in the Control WRF case. As an analogy, it might be equivalent to looking at a thermostat in a home, seeing that it was meeting the desired temperature, and concluding that the furnace was not activated in the previous hour. Of course, the furnace may have been on and that was why the desired temperature was met. CMAQ is using the profiles after the mixing has been accomplished within WRF (after the furnace being on), and thus its derived K s that are based on the mixed profiles coming from WRF have no need for mixing (turning on the furnace).

Thus, it was decided to examine the K values that would be produced by CMAQ from the two WRF runs. Rather

than rerunning CMAQ, the CMAQ code that computes the K s was extracted and used as a stand-alone code to compute the K s (using the WRF output) as CMAQ would do. Figure 18 shows the difference in the CMAQ diagnosed K s for an overwater cross section. Figure 19 shows traditional profiles of the diagnosed K s. The figure demonstrates that the re-diagnosed K s in CMAQ are consistently larger for the ACM2 case than for the Louis case. These results confirm that the WRF Model with larger mixing actually produces smaller re-diagnosed mixing coefficients in CMAQ.

These results show that in fact the CMAQ diagnosed K s from the Louis case are actually smaller than the K s from the ACM2 case. With this information, it can tentatively be concluded that the higher surface concentrations seen in the Louis enhanced-mixing case may in fact be due to less mixing in CMAQ. This would also be consistent with the view that CMAQ overprediction was due to not enough mixing. Thus, it appears that the 2009 CMAQ was driven by a meteorological model (NAM) that had too much vertical mixing. This counterintuitively may have led to smaller amounts of mixing in CMAQ. The overprediction in the 2009 CMAQ relative to the ferry observations may

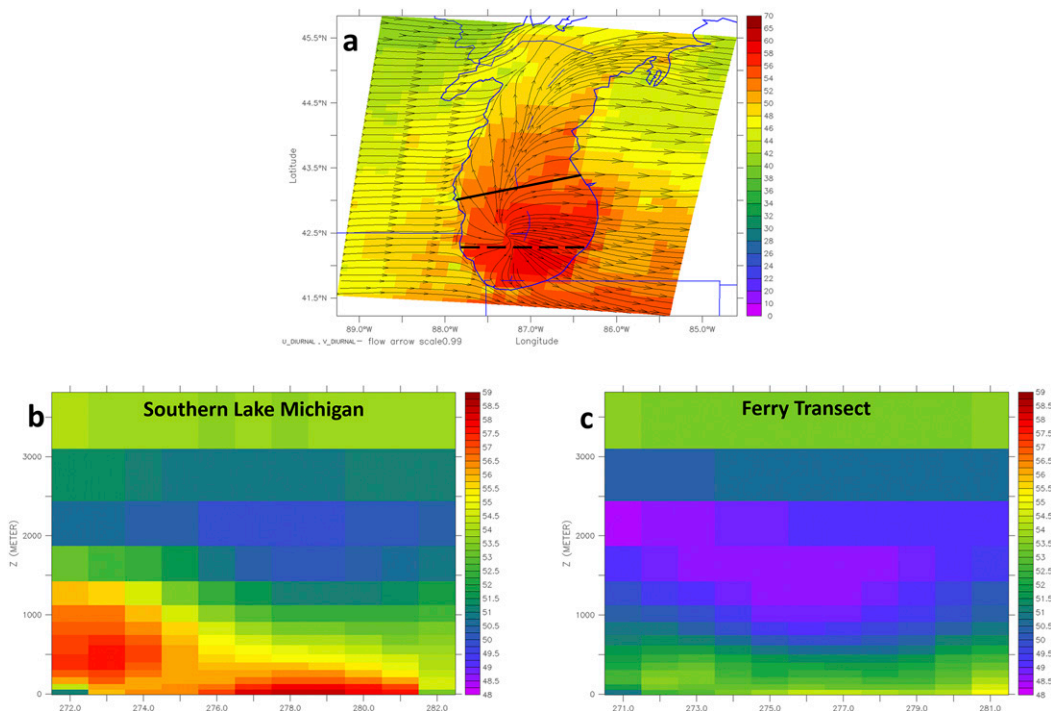


FIG. 14. As in Fig. 13, but for 1300 local time. Note that the highest levels of ozone are near the surface in the eastern part of the lake.

be partly due to smaller mixing in CMAQ caused by the well-mixed profiles coming from NAM.

3. Improvement in model prediction of temperatures in the Great Lakes region

As noted earlier, temperature affects emissions, chemistry, and vertical mixing. In the Great Lakes region, however, the evolving land surface temperatures and their contrast with the lake temperatures also drive the lake- and land-breeze regimes. Land surface temperatures are largely controlled by solar energy input and the characteristics of the land surface, which partition outgoing energy into sensible and evaporative fluxes (Wetzel et al. 1984; McNider et al. 1994) and to the thermal inertia of the land surface (Carlson 1986; McNider et al. 2005). Aside from its impact on temperatures, the partitioning of solar energy into evaporative fluxes from vegetation is also critical for air quality since stomatal uptake of ozone is one of the major loss terms in the ozone budget (Pleim et al. 2001).

Because of the importance of the characteristics of the land surface, there has been tremendous investment by the climate, weather forecasting, and air quality communities in land surface research. Much of this investment has gone into developing complex land surface

models, which include many intricate parameterizations that attempt to capture processes such as plant transpiration rates, leaf water interception, soil moisture and runoff, and parameterizations that control thermal and water transfer through canopies and soils (Sellers et al. 1997; Pitman 2003). Thus, these models require additional parameter specifications to close the model systems.

The use of satellite data (with observations such as greenness and albedo) has greatly improved the classification of the surface. However, land surface models in WRF (Chen and Dudhia 2001) do not use land-use classifications directly. Rather, they use physical parameters such as roughness, heat capacity, canopy thermal and water resistances, soil conductivity for water and heat, and so on that are associated with the land-use classes. Thus, in models, such as the WRF-Noah land-use model, there are lookup tables that define these land-use associated parameters (Niu et al. 2011).

Unfortunately, the specification of some of these physical parameters is difficult even in homogeneous land-use classes (Rosero et al. 2009). For example, the rate of temperature change in vegetation is controlled by plant transpiration and evaporation through water resistance parameters and by the canopy thermal resistance.

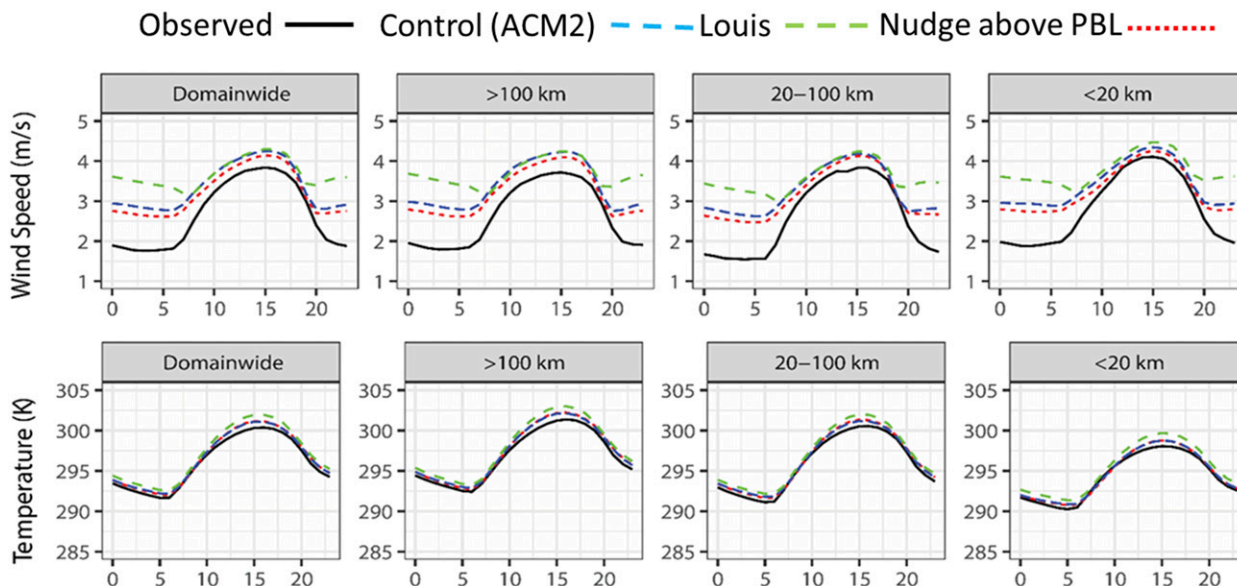


FIG. 15. WRF Model performance for land sites with the ACM2 (blue) and Louis adjustments to ACM2 (green). Both the ACM2 and Louis cases only nudged winds above 2 km. The nudging case (red line) applies to the ACM2 case but with nudging applied above the diagnosed boundary layer height, which can be below 2 km.

Thermal resistance depends on the heat capacity of the canopy and the thermal conductivity through the canopy (Noilhan and Planton 1989). The water resistance depends on root zone moisture, the phenological state of the plant-leaf area, shaded leaf area, and so on. Field campaigns using tower measurements are usually conducted to try to establish these parameters. However, in effect, many of the parameters or processes have to be deduced as residuals in local canopy models, which are tied to specific turbulence and radiative models (Yang and Friedl 2003; Pleim and Gilliam 2009). Thus, the parameters are often model heuristics as opposed to fundamental observables (Wagner and Gupta 2005), which is the reason a parameter such as canopy thermal resistance can vary by three orders of magnitude in different models (Pleim and Gilliam 2009). In inhomogeneous grid boxes, which make up the real world, the situation is even worse (McNider et al. 2005).

The development of complex land surface models mentioned above was consistent with the need in the climate modeling community for surface models that could be run for years without being influenced by observed data. Thus, they needed vegetative surface interaction, water balance models, etc. However, Diak (1990), McNider et al. (1994), Anderson et al. (1997), and others argued that for short-term weather forecasting and for retrospective air quality simulations (McNider et al. 1998; Pleim and Xiu 2003), simpler models that could be constrained by observations might be preferred. The simple models avoid setting many uncertain parameters

in the complex models. This is the path pursued here, with observational constraints provided by satellite skin-temperature data. Pleim and Xiu (2003) used the differences between observed analyses and model values of 2-m temperatures and 2-m surface relative humidity to adjust soil moisture. Here, the P-X surface data assimilation model (Pleim et al. 2001; Pleim and Xiu 2003) is modified to use satellite skin temperature rather than NWS-observed 2-m temperatures and humidity to adjust soil moisture and to recover the surface thermal resistance following McNider et al. (2005). Note that hereinafter NWS is used to denote surface observation, but this includes all surface observations in the DS472 used in WRF for surface data and not just NWS stations. Details on the modifications to P-X are given in the appendix.

A series of model experiments on a 12-km-resolution national domain were carried out employing these satellite assimilation techniques for month-long periods in 2012 and 2013 as well as use of satellite-derived insolation and satellite-derived greenness fraction. Geostationary Operational Environmental Satellite (GOES)-observed temperatures that are based on a single channel retrieval (Anderson et al. 2007a,b) rather than surface observations are used to adjust moisture [see Eq. (A4)]. Details on the satellite datasets and sequential inclusion of different satellite assimilation components are provided in McNider et al. (2017). Here we provide the impact of the satellite assimilation on temperatures and winds in the Great Lakes region.

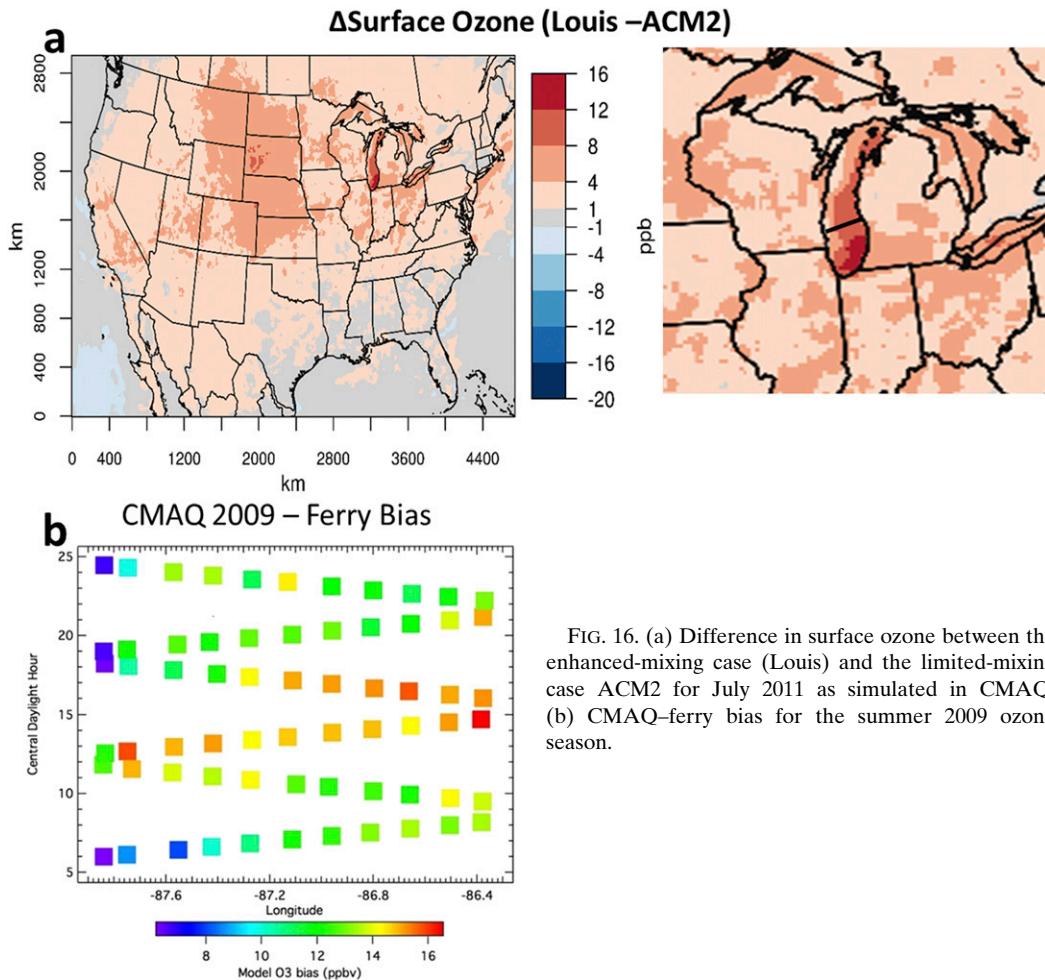


FIG. 16. (a) Difference in surface ozone between the enhanced-mixing case (Louis) and the limited-mixing case ACM2 for July 2011 as simulated in CMAQ. (b) CMAQ–ferry bias for the summer 2009 ozone season.

In carrying out the satellite assimilation, several satellite datasets were included.

- 1) Satellite-derived insolation (INSL): Incoming solar energy is a major component in the surface energy budget. However, models have difficulty getting clouds correct in space and time that control incoming energy. Here a technique to replace model-derived insolation with satellite-derived insolation (Gautier et al. 1980; McNider et al. 1995) is employed. Note that replacing the model insolation with the satellite insolation may introduce inconsistencies between the incoming energy and where the model has clouds. However, in trying to deduce moisture, having the correct input energy to the surface is critical. For example, if a grid cell actually has clouds but the model does not, then the moisture nudging would erroneously see a slow rise in temperature in the model as a need to add moisture. This would be a problem in both the P–X moisture nudging and the satellite moisture nudging. A better

solution would be for the model clouds to be more consistent with satellite clouds. A recent paper (White et al. 2018) that adjusts the model dynamics to support clouds shows progress in this regard.

- 2) Satellite-derived vegetation fraction (VEG): While satellite data have been employed to develop climatological greenness fractions such as in U.S. Geological Survey (USGS) land-use sets or NLCD, vegetative greenness varies annually and seasonally (Ran et al. 2016). A seasonal adjustment that is part of the P–X scheme gave erroneously high values, especially in the western United States (Ran et al. 2016). Here MODIS-derived greenness (Case et al. 2014) is employed in the P–X land surface scheme in a manner similar to that of Ran et al. (2016) for only the 2013 simulation.
- 3) Nudging of soil moisture using satellite skin temperatures (SM): Soil moisture was nudged using Eq. (A4) as opposed to the observed surface analyses originally employed in P–X [Eq. (A3)].

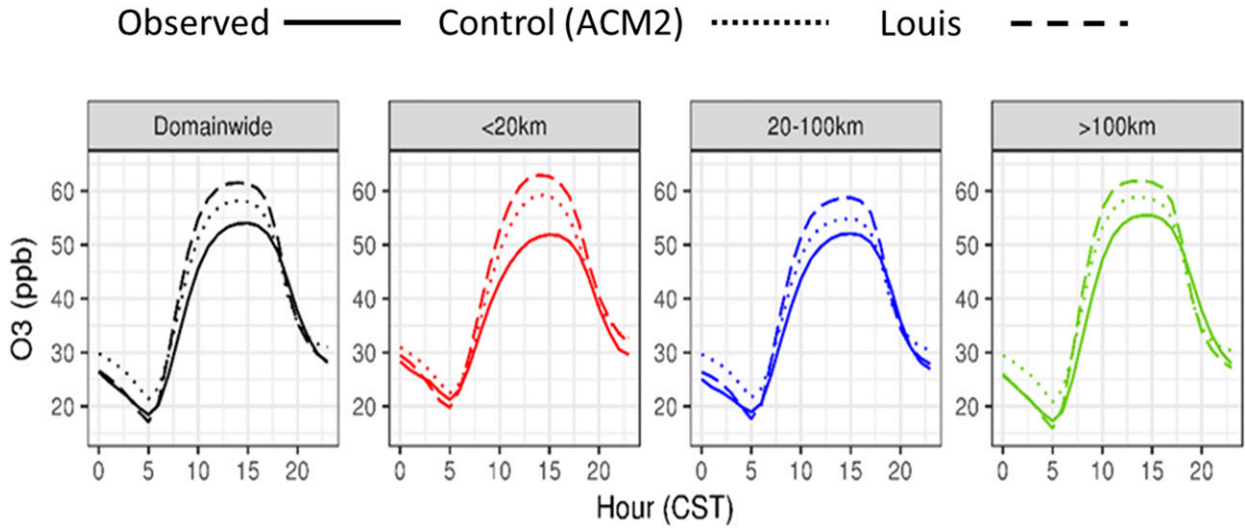


FIG. 17. Ozone performance statistics for the CMAQ ACM2 and Louis cases.

4) Adjustment of surface heat capacity (thermal inertia) using satellite skin temperatures (HC): As noted in sensitivity studies (Carlson 1986), the rate of temperature decline in the late afternoon and early evening is controlled by surface heat capacity. Here an adjustment is made to heat capacity using Eq. (A5) following McNider et al. (2005).

Figure 20 shows the diurnal evaluation in model performance due to the satellite assimilation for the Great Lakes region for the month of September 2013. Note that each successive case includes prior assimilation. For example, VEG includes satellite insolation and satellite vegetation, and HC includes all the assimilations (INSL, VEG, and SM). Figure 20 shows that during the daytime successive assimilation of INSL, VEG, and SM improves

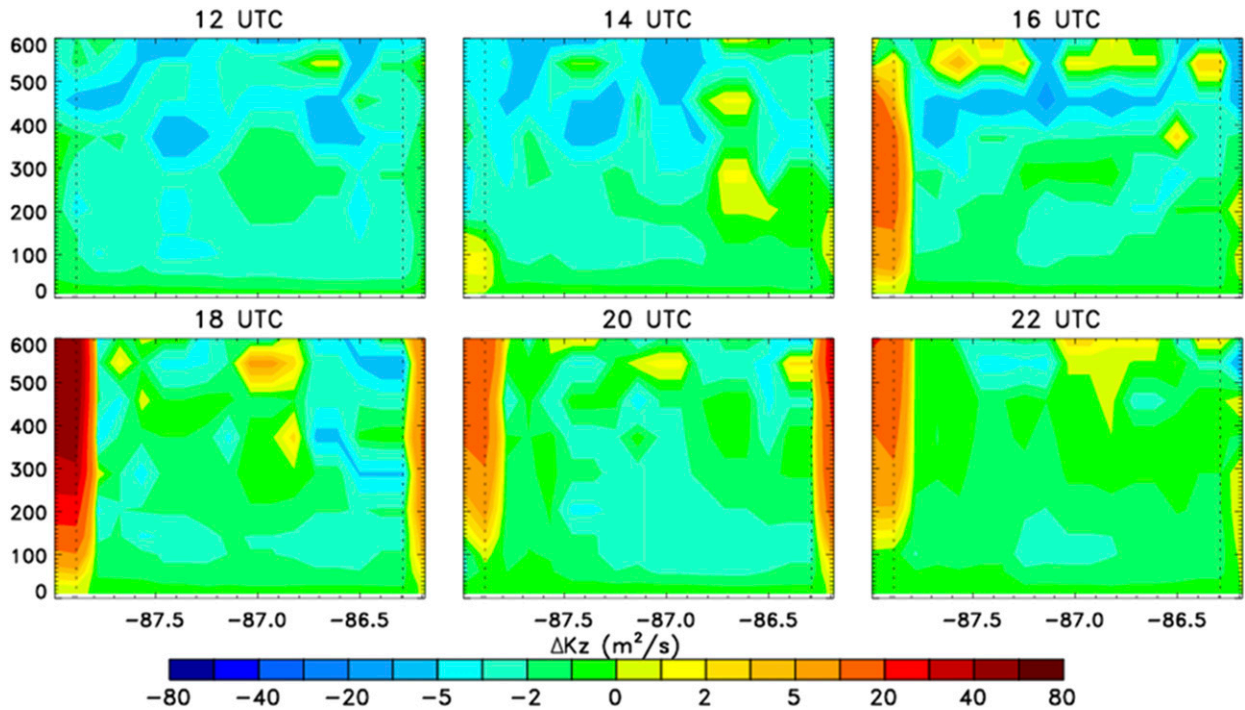


FIG. 18. Difference (Louis – ACM2) in vertical mixing coefficients K diagnosed in CMAQ. Note that Louis K s are smaller than ACM2 K s. Dashed lines give the longitudes of the ferry ports.

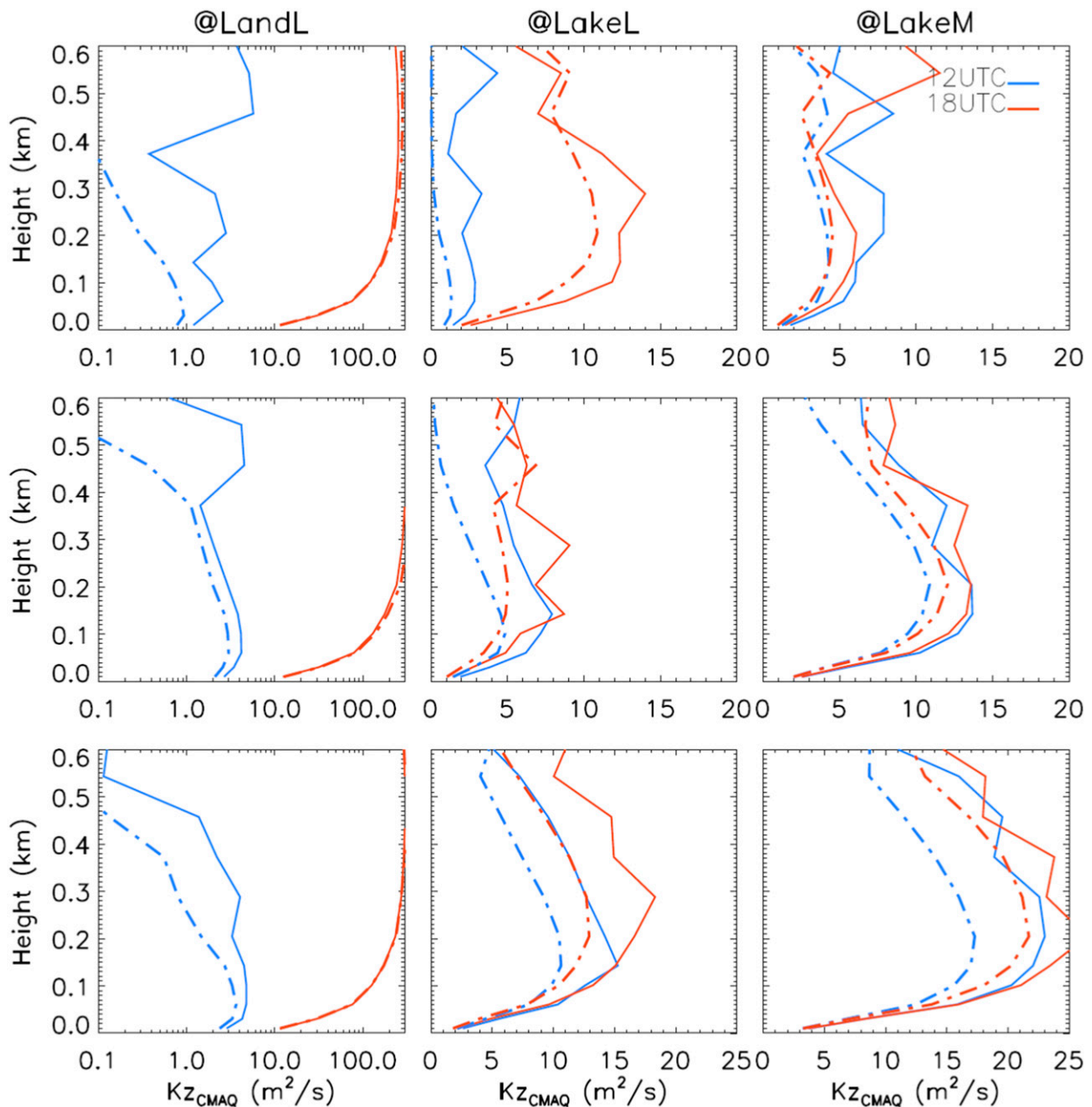


FIG. 19. Vertical profiles of K diagnosed in CMAQ for the ACM2 and Louis WRF cases for (top) the cross section 1° of latitude north of the ferry path, (middle) the cross section near the ferry transect, and (bottom) the cross section 1° of latitude south of the ferry transect for (left) a land point on the western shore, (right) a point in the middle of the lake, and (center) for a point between them. The solid lines are for the ACM2 case (small mixing), and dash-dotted lines are for the Louis case (large mixing). Blue is for 1200 UTC, and red is for 1800 UTC. Note that the rediagnosed K s in CMAQ are consistently larger for the ACM2 case than for the Louis case.

bias in 2-m temperature. In this case, the soil moisture nudging adds moisture to the surface and reduces the temperature. At night, however, the SM (red curve) shows deterioration in performance. This is due to the added ground moisture, which increases the soil heat capacity so that temperatures do not cool as much at night. However, the HC, using afternoon and

early evening skin temperature, tries to correct heat capacity to a smaller value. Because of stability concerns within the solver, limits were placed on how much the heat capacity could be changed. It is possible that this can be relaxed/improved in the future through either filtering or higher-order solvers such as multipoint Runge–Kutta methods.

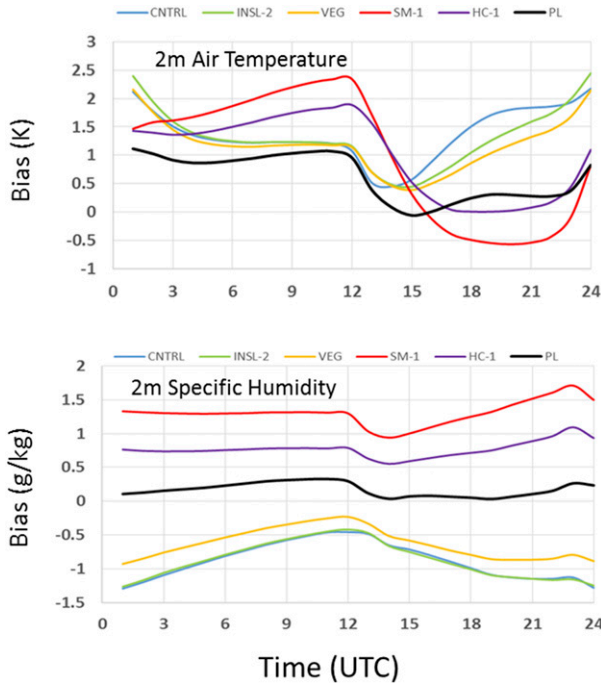


FIG. 20. Diurnal model bias of 2-m (top) temperature and (bottom) humidity at NWS sites in the Midwest domain due to satellite assimilation for September 2013. Label “CNTRL” (blue) gives base performance P–X with no satellite assimilation or NWS nudging. INSL-2 (green) shows the response of using satellite-derived insolation rather than model insolation. VEG (orange) shows the impact of using satellite greenness. SM (red) shows the impact of soil moisture nudging. HC (purple) shows the impact of heat capacity adjustment. Note that all satellite cases are cumulative (i.e., HC includes insolation, vegetation, soil moisture, and heat capacity). PL (black) gives the P–X with NWS nudging.

The label “CNTRL” in Fig. 20 is the P–X scheme but without the Pleim observational nudging employed. Figure 20 also shows the performance of the P–X scheme with NWS nudging, denoted as PL. As can be seen, the satellite HC case compares very favorably to PL in the daytime. In terms of humidity, the PL does slightly better than the satellite HC case. Remember that the PL uses both humidity and temperature in its moisture nudging approach, which may be an advantage over the satellite technique.

Table 5 provides a summary of the statistics. The 2-m temperature bias was improved by over a full degree and RMSE by about 0.8 K in the final simulations (HC). The 10-m wind speed performance was mixed, with bias slightly increasing and RMSE slightly decreasing. The assimilation reversed a dry bias to give a moist bias.

Figure 20 provides the performance at the observation sites that are used as data for moisture and deep temperature nudging. The reason for using satellite data is that they can capture spatial land-use information

beyond that of the local surface data. The satellite skin temperature can provide another metric. Model comparison with satellite observed skin temperatures also showed improvement for both satellite and P–X surface nudging cases (Table 6). Figure 21 (top) shows the diurnal bias in skin temperature (model minus satellite skin temperature) at surface observation sites and Fig. 21 (bottom) shows improvement for all grid points in the Midwest domain. The performance is not that different but with the satellite assimilation showing slightly better performance than at just the NWS observed surface sites. The Midwest is perhaps unique in that it has a higher concentration of surface observing sites than other regions, perhaps because of the agricultural interest, and land use is generally more homogeneous.

Overall, the satellite assimilation significantly improved the model 2-m temperature prediction. Figure 22 provides a spatial plot of model bias difference for the full satellite assimilation in the Great Lakes area and shows that at most observation sites model performance has been improved with some sites in the Corn Belt (southern Minnesota and Wisconsin, Iowa, Illinois, and Indiana) by several degrees. Improvement is especially consistent on the western and eastern shores of Lake Michigan. The 10-m wind speed performance due to the assimilation was mixed throughout the domain (not shown).

Similar experiments were carried out for 2012. While September 2013 discussed above was somewhat dry in the Midwest, it and the rest of the country had been relatively moist prior to late summer. However, 2012 was an extraordinary drought for most of the summer. Figure 23 shows the diurnal statistical evaluation for the satellite assimilation and P–X NWS nudging performed for the month of August 2012. It shows that the Control simulation was extraordinarily warm relative to observations. Both the satellite assimilation and P–X moisture nudging moistened the atmosphere and improved the performance. The P–X with nudging is remarkable in its improvement of 2-m temperature and moisture. In 2013 the satellite assimilation was competitive with the P–X nudging; however, in 2012, the satellite technique appears to overadjust moisture, making the moisture too high and overcooling the atmosphere. This is an issue that requires further investigation and may in part be due to model quality assurance/quality control (QA/QC) procedures that were relaxed in 2012. For the 2013 case, to avoid possible contamination in skin temperatures and to avoid issues with longwave radiation from model clouds interfering within the surface energy budget, an aggressive technique was employed to bypass the moisture adjustment

TABLE 5. Bias (-B) and RMSE (-R) for 2-m temperature (T2M), 2-m specific humidity (Q2M), and 10-m wind speed (WSPD10M) at standard NWS observations sites over the Great Lakes domain for various WRF simulations (12-km grid spacing; daytime conditions for 1–30 Sep 2013).

Run	T2M-B	Q2M-B	WSPD10M-B	T2M-R	Q2M-R	WSPD10M-R
Control	1.325	-0.932	-0.245	2.838	2.259	2.615
INSL	1.157	-0.940	-0.282	2.557	2.234	2.555
VEG	0.991	-0.710	-0.335	2.392	2.052	2.533
SM	0.112	1.289	-0.410	2.013	1.996	2.471
PL	0.273	0.118	-0.405	1.942	1.368	2.522
HC	0.472	0.765	-0.376	1.935	1.678	2.481

if either GOES clouds or model clouds were present. Clouds were determined on the basis of whether insolation values were less than 95% of clear-sky values. For some reason that we are still investigating, the cloud-rejection criteria basically removed almost all opportunities for moisture adjustments. To make moisture adjustments, the cloud-rejection test was completely removed. This removal may be a reason why the satellite assimilation did not perform as well in 2012 as in 2013. Also, the 2012 case did not include the satellite vegetation replacement since the product used in 2013 was not available. An examination of GOES satellite data showed that the dryness in the present Control model had many fewer clouds than were observed by the satellite. The lack of clouds in the model is apparently a feedback of having an atmosphere with relative humidity far too low to support cloud development.

The initial dry bias in the model emanates from model initialization based on the large-scale NAM-12 analysis but is continued in the Control case. This points to what may be a consistent problem in land surface models, especially in normally moist regions. It appears that land surface models perhaps perform well in the eastern United States when precipitation dominates the moisture budget but may do poorly when the moisture budget is controlled by nonobserved parameters such as canopy resistance, soil moisture diffusion, and so on. Ukkola et al. (2016) tested 14 land surface model (LSM) versions against in situ data and tower data. Using three metrics, they found that the models during evaporative drought conditions consistently overestimated the duration, magnitude and intensity of drought. They concluded that their “findings point to systematic biases across LSMs when simulating water and energy fluxes under water-stressed conditions.” Thus, in air quality studies where hot and dry conditions often coincide with extreme air quality events, there may be concern that land models may overstate these conditions. This is apparently the case in 2012 for the Midwest. It points to a need to have moisture corrections such as the P-X observational nudging or the satellite data technique to bring moisture back to reasonable values.

4. Summary and conclusions

This paper addresses aspects of the average physical atmosphere and issues with modeling the atmosphere in the Great Lakes region for multiple years.

a. Overwater overprediction of ozone over Lake Michigan

It appears that there is relatively little difference in performance of the different widely used PBL schemes in WRF 3.8.1 in the stable boundary layer for the 2009 simulations. All give similar overwater performance compared to buoys, and their temperature and wind profiles over water are also similar. It appears that the NAM-12 operational model used in the 2009 operational CMAQ [which showed overprediction of ozone compared to ferry data in Cleary et al. (2015)] has less-stable profiles and less surface wind shear than the WRF 3.8.1 profiles. The source of these less-stable profiles in the operational 2009 NAM-12 is unclear since it employed the MYJ scheme that showed more-stable profiles in the WRF 3.8.1.

A CMAQ mixing sensitivity run was designed to test the impact of mixing on surface ozone. A new WRF 3.8.1 case that was configured to have more mixing (the Louis case) produced long-term average 2009 wind and temperature profiles that were similar to the operational 2009 NAM-12 as seen in the CMAQ meteorological files. This configuration was then used to make a July 2011 WRF 3.8.1 run. In turn, this was used to drive a CMAQ run. It was found that the increased mixing WRF run produced higher surface ozone over Lake Michigan. However, further investigation showed that the rediagnosed mixing coefficients in CMAQ were actually less than the CMAQ driven by the Control WRF. Thus, it is concluded that the increased surface concentrations in the 2011 CMAQ were due to decreased mixing. Applying these findings to the 2009 CMAQ-vs-ferry overprediction issue, we conclude that the overprediction could have been caused by too much mixing in the NAM meteorological model, which translated into too little mixing in the operational CMAQ. Future modelers should be

TABLE 6. Bias (-B) and RMSE (-R) for skin temperature for various WRF simulations from the 12-km grid for the Great Lakes domain for daytime conditions for 1–30 Sep 2013.

Run	TSKIN-B	TSKIN-R
Control	2.761	4.591
INSL	3.307	4.894
VEG	2.796	4.453
SM	0.379	3.134
PL	1.288	3.084
HC	1.016	3.257

wary of this issue, and it is recommended that WRF be run with the ACM2 scheme that is employed in CMAQ. However, even here the use of offline meteorology can possibly lead to differences in the mixing in the stable boundary layer. This is because the wind and temperature profiles passed to CMAQ reflect past mixing that may not be found in the rediagnosed mixing coefficients.

b. Improvement in model performance for the Great Lakes region using satellite assimilation in the P–X land surface model

A series of satellite assimilation experiments were carried out for the month of September 2013 and August 2012. The experiments showed that the assimilation of satellite products (insolation, vegetative fraction, and skin temperature for moisture and heat capacity adjustments) did improve model performance for both NWS metrics and satellite skin-temperature metrics in 2013 and 2012. The 2012 case is one in which the Control case (no satellite assimilation) had very large temperature and humidity errors relative to other years.

The large dry surface moisture errors in the 2012 and 2013 and in the surface moisture in the NAM-12 reanalysis during drought periods indicate perhaps an endemic problem with land surface models as discussed by Ukkola et al. (2016). In the absence of precipitation controlling the surface moisture budget, ill-specified unobserved parameters in the surface models may drive the solution to a too-dry and too-warm surface. Schemes such as the P–X soil moisture nudging using surface observation or the experimental satellite technique tested here may be needed in these dry cases.

c. Implications for air quality

The analysis above, that too much mixing in the NAM meteorological model driving operational CMAQ may result in increased overwater ozone, should perhaps be investigated by the NOAA air quality team. In examining NAM operational performance statistics for

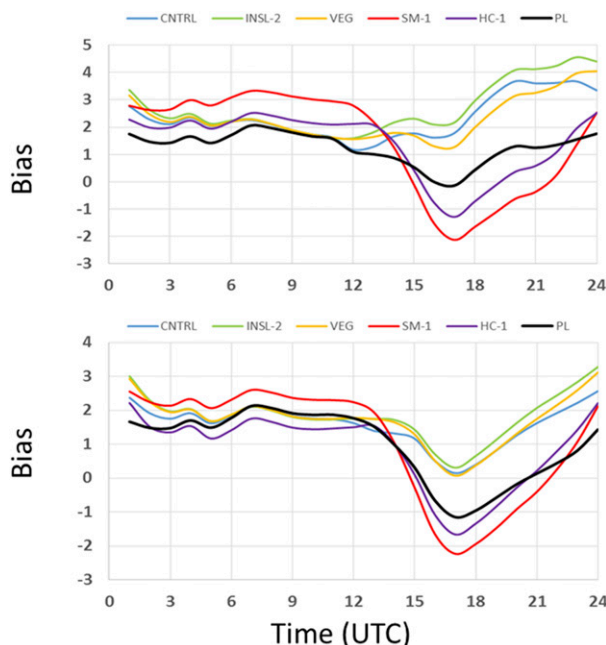


FIG. 21. Average bias of skin temperature (WRF diagnosed value minus GOES observed) for each UTC hour for various WRF simulations for the Great Lakes domain for September 2013 with (top) calculations performed only at DS472 surface observation locations and (bottom) calculations performed for all 12-km land WRF grid points. Label CNTRL (blue) gives base performance P–X with no satellite assimilation or NWS nudging. INSL (green) shows the response of using satellite-derived insolation rather than model insolation. VEG (orange) shows the impact of using satellite greenness. SM (red) shows the impact of soil moisture nudging. HC (purple) shows the impact of heat capacity adjustment. PL (black) gives the P–X with NWS nudging. Note that the satellite cases are cumulative (i.e., HC includes insolation, vegetation, soil moisture nudging, and heat capacity adjustment).

August 2010 to the present for the Great Lakes region (see the very useful operational evaluation site <http://www.emc.ncep.noaa.gov/mmb/research/nearsfc/nearsfc.verf.html>) it appears that surface wind speeds are greatly overestimated especially at night (in terms of percent error) from 2010 to the present, indicating perhaps a continuing overmixing of momentum to the surface. While model output statistics (MOS) may make this persistent bias not an issue in the operational forecasting world, the unadjusted wind speed errors in an air quality model may be a problem.

Improvements in temperatures may also change ozone NO_x sensitivity. As noted by Sillman (1995), the thermal decomposition of nitrogen species can allow longer chemical chain lengths and alter the slope of ozone– NO_y relationships. The large overprediction of temperature in 2012 would produce a system in which NO_y sensitivity is larger than reality because NO_x can reenter the system through excessive thermal decomposition.

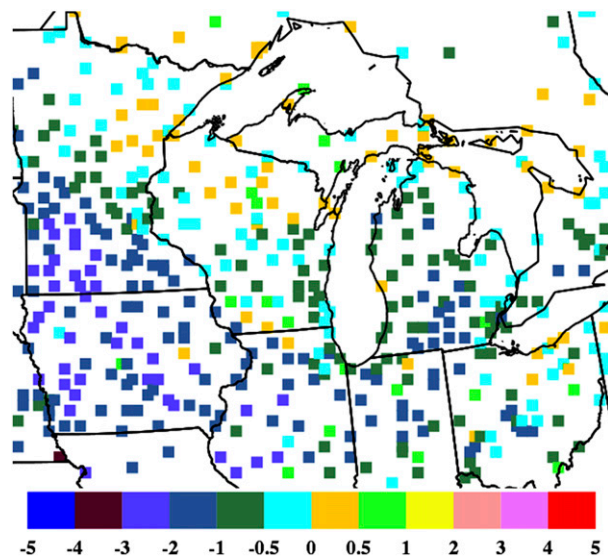


FIG. 22. Spatial plot of impact on NWS sites from satellite assimilation for 2013 for the soil moisture assimilation case. The plot shows the difference in magnitude of the bias between the Control run and the heat capacity run (HC) for daytime hours. Negative values indicate improvement. Note that the HC case includes insolation, vegetation, soil moisture nudging, and heat capacity adjustments. Values are truncated to the range ± 5 K.

Additional natural and evaporative hydrocarbons would be supported by the higher erroneous temperatures as well.

The consistent surface wind speed overprediction in the 2009 model especially at night and early morning is troubling (in a general sense but not as an explanation of the overwater overprediction) in that the surface wind speed controls the initial conversion of emissions to volumetric concentrations. If surface wind speeds are overpredicted by 30%–50%, this means emissions are being overdiluted, giving erroneously low ambient concentrations. Today measurements of precursors or products such as NO_x or NO_y are sometimes used to assess the quality of emissions. However, if ambient measurements are used to evaluate emission values, a wind speed overprediction would look like an underestimate of emissions.

The significant lack of model clouds in the 2012 Control case versus observed is also of concern. Clouds not only impact temperatures, as presented here, but also they modulate photolysis rates (Pour-Biazar et al. 2007). The year 2012 provided one of the most severe ozone episodes in most of the Midwest in recent years (<https://www.epa.gov/air-trends/trends-ozone-adjusted-weather-conditions>). If chemical model simulations were carried out for the 2012 period with the Control case model-based clouds it would greatly overstate photolysis rates.

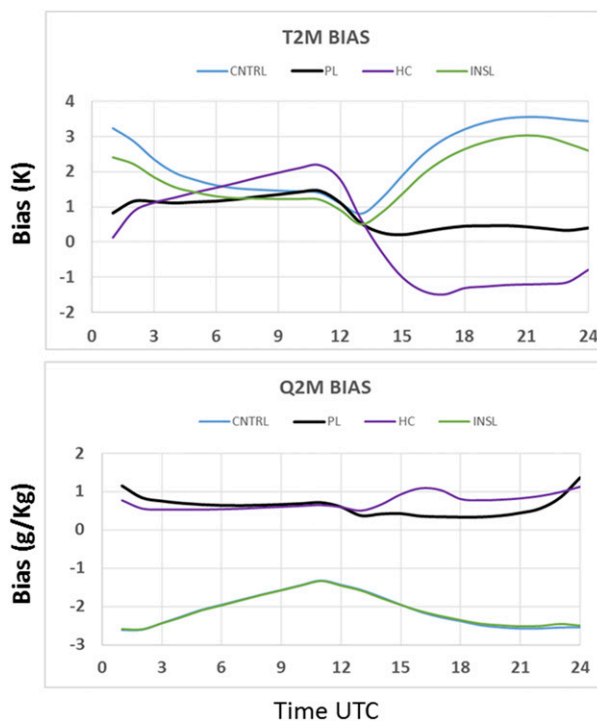


FIG. 23. Diurnal model bias of 2-m temperature and humidity at sites in the Midwest domain from satellite assimilation for August 2012. Label CNTRL (blue) gives base performance with no satellite assimilation or surface nudging. INSL (green) shows the response of using satellite-derived insolation rather than model insolation. HC (purple) shows the impact of heat capacity adjustment. PL shows the P-X with NWS nudging. Note that all cases are cumulative (i.e., HC includes insolation, soil moisture, and heat capacity).

d. Future modeling and observations

It is hoped that this work can help to interpret future meteorological modeling in the Great Lakes region supporting future observational campaigns and air quality management. Given the 2009 work discussed above, it would be very useful to reimplement the continuous ferry observations. The lack of clouds in the 2012 case indicates that either replacement of model clouds by satellite clouds (Pour-Biazar et al. 2007) or new satellite cloud assimilation strategies (White et al. 2018) may be important for model fidelity.

Acknowledgments. This research was sponsored in part by the Electric Power Research Institute (EPRI), the State of Texas Air Quality Research Program (AQRP), and the NASA Applied Sciences Program. The findings in this research do not necessarily reflect the views of EPRI or NASA or those of the AQRP or the Texas Commission on Environmental Quality.

Note that the results in this study do not necessarily reflect policy or science positions by the funding agencies. We thank program managers John Haynes, Eladio Knipping, and Elena McDonald for their support.

APPENDIX

Description of Code Modifications

a. Adjustments to ACM2 (PBL case)

Although they were minor, the ACM2 as constituted in WRF 3.8.1 contained a few adjustments that could potentially increase mixing. Components that were modified are provided below.

- 1) The ACM2 scheme employs a stability function in the stable boundary layer to specify vertical diffusion coefficients for momentum and heat (K_m ; K_h) as in Eq. (A1):

$$K_h = f(\text{Ri})l^2s \quad \text{and} \quad K_m = K_h P_R, \quad (\text{A1})$$

where P_R is the Prandtl number = 0.8, Ri is the Richardson number, l is a mixing length, and s is the wind shear. ACM2 employs a polynomial form for the stability function $f(\text{Ri})$. The ACM2 stability function (Pleim polynomial) has slightly more mixing than the England–McNider quadratic stability function, which is derived on the basis of Monin–Obukov similarity (England and McNider 1995). Here the England–McNider form (an even-shorter-tailed form) replaced the ACM2 stability functions for stable conditions.

- 2) A mesoscale enhancement, dependent on horizontal resolution, in u_* was removed.
- 3) Some minimum values for u_* were made smaller.

b. Surface-layer adjustments for the Louis case

In creating the Louis case, surface fluxes were also modified in a manner similar to England and McNider (1995),

$$u_*^2 = \kappa^2 f_m(\text{Ri}_{1/2}) |V_1^2| / \ln(z_1/z_0) \quad \text{and} \\ u_* \Theta_* = \kappa^2 f_h(\text{Ri}_{1/2}) |V_1| |(\Theta_1 - \Theta_g)| / \ln(z_1/z_0), \quad (\text{A2})$$

where u_* is the surface friction velocity, $u_* \Theta_*$ is the surface heat flux, κ is the von Kármán constant, V_1 is the model first-level wind speed, Θ_1 is the first-level temperature, and Θ_g is the ground temperature. The stability functions f_h and f_m were taken to be the Louis

stability functions as seen in Fig. 3. Note that this is a modification to the ACM2/P–X schemes to give more mixing and is not exactly the original Louis (1979) boundary layer scheme.

c. Pleim–Xiu moisture nudging

Pleim and Xiu (2003) noted that, since surface moisture is not directly observed, use of auxiliary information is needed. Considering energetics, they have used observed surface temperature and relative humidity to nudge moisture. As shown in Eq. (A3) below, they adjust surface-layer moisture w_G using the difference between model daytime temperatures T^F and analyses of observed temperatures T^A and model and observed relative humidity RH :

$$\Delta w_G = \alpha_1(T^A - T^F) + \alpha_2(\text{RH}^A - \text{RH}^F), \quad (\text{A3})$$

where $\alpha_{1,2}$ are nudging coefficients. A similar equation is also used by Pleim and Xiu (2003) to nudge the deep-layer soil moisture, which may be more important than surface moisture, especially in vegetated areas. The P–X approach has been widely used and in recent California intercomparisons performed better than the Noah complex land surface model (Fovell 2013). Because surface observations are sparse, here they are replaced with higher-resolution satellite skin temperatures. It is hoped that this can capture finescale land-use characterizations that are not seen in the coarser surface observations. The satellite skin temperatures are included as

$$\Delta w_G = \beta_1(T_s^{\text{Sat}} - T_s^{\text{Mod}})_{\text{Morning}}. \quad (\text{A4})$$

Here T_s^{Sat} is the satellite observed skin temperature, T_s^{Mod} is the modeled skin temperature, and β_1 is a nudging coefficient, set to $5.56 \times 10^{-7} \text{ m s}^{-1} \text{ K}^{-1}$ in these simulations. Deep soil moisture is also nudged in a similar fashion. Heat capacity can also be adjusted as in Eq. (A5):

$$C_T^{\text{NEW}} = C_T^{\text{OLD}} \left(\frac{\partial T_s^{\text{SAT}}}{\partial t} / \frac{\partial T_s^{\text{MOD}}}{\partial t} \right). \quad (\text{A5})$$

For further details on implementation and testing, see Mackaro et al. (2011) and McNider et al. (2005). Note that the use of skin temperatures is consistent with the P–X energetic assumption that moisture is related to 2-m temperatures, and this formulation makes the same assumption for skin temperature. The technique proposed by McNider et al. (2005) is employed within the P–X model to nudge thermal resistance C_T using afternoon/evening skin temperatures [as opposed to the Pleim and Gilliam (2009) technique of using

afternoon/evening temperatures to nudge deep soil temperature] as illustrated by Eqs. (A3)–(A5).

REFERENCES

- Adamski, W., 2003: Using aircraft-based ozone and oxide of nitrogen measurements to estimate aloft ozone responsiveness to precursor levels. Wisconsin Department of Natural Resources, Bureau of Air Management Publ. AM-336-2003.
- Anderson, M. C., J. M. Norman, G. R. Diak, W. P. Kustas, and J. R. Mecikalski, 1997: A two-source time-integrated model for estimating surface fluxes using thermal infrared remote sensing. *Remote Sens. Environ.*, **60**, 195–216, [https://doi.org/10.1016/S0034-4257\(96\)00215-5](https://doi.org/10.1016/S0034-4257(96)00215-5).
- , —, J. R. Mecikalski, J. A. Otkin, and W. P. Kustas, 2007a: A climatological study of evapotranspiration and moisture stress across the continental United States based on thermal remote sensing: 1. Model formulation. *J. Geophys. Res.*, **112**, D10117, <https://doi.org/10.1029/2006JD007506>.
- , —, —, —, and —, 2007b: A climatological study of evapotranspiration and moisture stress across the continental United States based on thermal remote sensing: 2. Surface moisture climatology. *J. Geophys. Res.*, **112**, D11112, <https://doi.org/10.1029/2006JD007507>.
- Appel, W., R. Gilliam, J. Pleim, G. Pouliot, D.-C. Wong, C. Hogrefe, S. Roselle, and R. Mathur, 2014: Improvements to the WRF–CMAQ modeling system for fine-scale air quality simulations. *EM Magazine*, Vol. 14, Air & Waste Management Association, Pittsburgh, PA, 16–21.
- Banta, R. M., and Coauthors, 2005: A bad air day in Houston. *Bull. Amer. Meteor. Soc.*, **86**, 657–669, <https://doi.org/10.1175/BAMS-86-5-657>.
- , and Coauthors, 2011: Dependence of daily peak O₃ concentrations near Houston, Texas on environmental factors: Wind speed, temperature, and boundary-layer depth. *Atmos. Environ.*, **45**, 162–173, <https://doi.org/10.1016/j.atmosenv.2010.09.030>.
- Beljaars, A. C. M., and A. A. M. Holtslag, 1991: Flux parameterization over land surfaces for atmospheric models. *J. Appl. Meteor.*, **30**, 327–341, [https://doi.org/10.1175/1520-0450\(1991\)030<0327:FPOLSF>2.0.CO;2](https://doi.org/10.1175/1520-0450(1991)030<0327:FPOLSF>2.0.CO;2).
- Blackadar, A. K., 1979: High resolution models of the planetary boundary layer. *Advances in Environmental Sciences and Engineering*, J. R. Pfafflin and E. N. Ziegler, Eds., Vol. 1, Gordon and Breach, 50–85.
- Bosveld, F. C., and Coauthors, 2014: The third GABLS intercomparison case for evaluation studies of boundary-layer models. Part B: Results and process understanding. *Bound.-Layer Meteor.*, **152**, 157–187, <https://doi.org/10.1007/s10546-014-9919-1>.
- Businger, J. A., 1973: Turbulent transfer in the atmospheric surface layer. *Workshop on Micrometeorology*, D. A. Haugen, Ed., Amer. Meteor. Soc., 67–100.
- Byun, D., and K. L. Schere, 2006: Review of the governing equations, computational algorithms, and other components of the Models-3 Community Multiscale Air Quality (CMAQ) modeling system. *Appl. Mech. Rev.*, **59**, 51–77, <https://doi.org/10.1115/1.2128636>.
- Carlson, T. N., 1986: Regional scale estimates of surface moisture availability and thermal inertia using remote thermal measurements. *Remote Sens. Rev.*, **1**, 197–246, <https://doi.org/10.1080/02757258609532069>.
- Case, J. L., F. J. LaFontaine, J. R. Bell, G. J. Jedlovec, S. V. Kumar, and C. D. Peters-Lidard, 2014: A real-time MODIS vegetation product for land surface and numerical weather prediction models. *IEEE Trans. Geosci. Remote Sens.*, **52**, 1772–1786, <https://doi.org/10.1109/TGRS.2013.2255059>.
- Chen, F., and J. Dudhia, 2001: Coupling an advanced land surface–hydrology model with the Penn State–NCAR MM5 modeling system. Part I: Model implementation and sensitivity. *Mon. Wea. Rev.*, **129**, 569–585, [https://doi.org/10.1175/1520-0493\(2001\)129<0569:CAALSH>2.0.CO;2](https://doi.org/10.1175/1520-0493(2001)129<0569:CAALSH>2.0.CO;2).
- Cleary, P. A., and Coauthors, 2015: Ozone distributions over southern Lake Michigan: Comparisons between ferry-based observations, shoreline-based DOAS observations and model forecasts. *Atmos. Chem. Phys.*, **15**, 5109–5122, <https://doi.org/10.5194/acp-15-5109-2015>.
- Diak, G. R., 1990: Evaluation of heat flux, moisture flux and aerodynamic roughness at the land surface from knowledge of the PBL height and satellite-derived skin temperatures. *J. Agric. For. Meteor.*, **52**, 181–198, [https://doi.org/10.1016/0168-1923\(90\)90105-F](https://doi.org/10.1016/0168-1923(90)90105-F).
- Dye, T. S., P. T. Roberts, and M. E. Korc, 1995: Observations of transport processes for ozone and ozone precursors during the 1991 Lake Michigan Ozone Study. *J. Appl. Meteor.*, **34**, 1877–1889, [https://doi.org/10.1175/1520-0450\(1995\)034<1877:OOTPFO>2.0.CO;2](https://doi.org/10.1175/1520-0450(1995)034<1877:OOTPFO>2.0.CO;2).
- Eder, B., D. Kang, R. Mathur, J. Pleim, S. Yu, T. Otte, and G. Pouliot, 2009: A performance evaluation of the National Air Quality Forecast Capability for the summer of 2007. *Atmos. Environ.*, **43**, 2312–2320, <https://doi.org/10.1016/j.atmosenv.2009.01.033>.
- Ek, M. B., K. E. Mitchell, Y. Lin, E. Rogers, P. Grunmann, V. Koren, G. Gayno, and J. D. Tarpley, 2003: Implementation of Noah LSM advances in the National Centers for Environmental Prediction operational mesoscale Eta Model. *J. Geophys. Res.*, **108**, 8851, <https://doi.org/10.1029/2002JD003296>.
- England, D. E., and R. T. McNider, 1995: Stability functions based upon shear functions. *Bound.-Layer Meteor.*, **74**, 113–130, <https://doi.org/10.1007/BF00715713>.
- Fast, J. D., and W. E. Heilman, 2003: The effect of lake temperatures and emissions on ozone exposure in the western Great Lakes region. *J. Appl. Meteor.*, **42**, 1197–1217, [https://doi.org/10.1175/1520-0450\(2003\)042<1197:TEOLTA>2.0.CO;2](https://doi.org/10.1175/1520-0450(2003)042<1197:TEOLTA>2.0.CO;2).
- Foley, T., E. A. Betterton, P. R. Jacko, and J. Hillery, 2011: Lake Michigan air quality: The 1994–2003 LADCO Aircraft Project (LAP). *Atmos. Environ.*, **45**, 3192–3202, <https://doi.org/10.1016/j.atmosenv.2011.02.033>.
- Fovell, R., 2013: WRF performance issues in the San Joaquin Valley and Southern California. *Traversing New Terrain in Meteorological Modeling for Air Quality and Dispersion*, Davis, CA, California Air Resources Board.
- Garcia-Menendez, F., Y. Hu, and M. T. Odman, 2013: Simulating smoke transport from wildland fires with a regional-scale air quality model: Sensitivity to uncertain wind fields. *J. Geophys. Res. Atmos.*, **118**, 6493–6504, <https://doi.org/10.1002/jgrd.50524>.
- Gautier, C., G. R. Diak, and S. Mass, 1980: A simple physical model for estimating incident solar radiation at the surface from GOES satellite data. *J. Appl. Meteor.*, **19**, 1005–1012, [https://doi.org/10.1175/1520-0450\(1980\)019<1005:ASPMTE>2.0.CO;2](https://doi.org/10.1175/1520-0450(1980)019<1005:ASPMTE>2.0.CO;2).
- Goldberg, D. L., C. P. Loughner, M. Tzortziou, J. W. Stehr, K. E. Pickering, L. T. Marufu, and R. R. Dickerson, 2014: Higher surface ozone concentrations over the Chesapeake Bay than over the adjacent land: Observations and models from the DISCOVER-AQ and CBODAQ campaigns. *Atmos. Environ.*, **84**, 9–19, <https://doi.org/10.1016/j.atmosenv.2013.11.008>.

- Hong, S., Y. Noh, and J. Dudhia, 2006: A new vertical diffusion package with an explicit treatment of entrainment processes. *Mon. Wea. Rev.*, **134**, 2318–2341, <https://doi.org/10.1175/MWR3199.1>.
- Hu, X. M., P. M. Klein, and M. Xue, 2013: Evaluation of the updated YSU planetary boundary layer scheme within WRF for wind resource and air quality assessments. *J. Geophys. Res. Atmos.*, **118**, 10 490–10 505, <https://doi.org/10.1002/jgrd.50823>.
- Iacono, M. J., J. S. Delamere, E. J. Mlawer, M. W. Shephard, S. A. Clough, and W. D. Collins, 2008: Radiative forcing by long-lived greenhouse gases: Calculations with the AER radiative transfer models. *J. Geophys. Res.*, **113**, D13103, <https://doi.org/10.1029/2008JD009944>.
- Janjić, Z. I., 2003: A nonhydrostatic model based on a new approach. *Meteor. Atmos. Phys.*, **82**, 271–285, <https://doi.org/10.1007/s00703-001-0587-6>.
- Kain, J. S., 2004: The Kain–Fritsch convective parameterization: An update. *J. Appl. Meteor.*, **43**, 170–181, [https://doi.org/10.1175/1520-0450\(2004\)043<0170:TKCPAU>2.0.CO;2](https://doi.org/10.1175/1520-0450(2004)043<0170:TKCPAU>2.0.CO;2).
- Keen, C. S., and W. A. Lyons, 1978: Lake/land breeze circulations on the western shore of Lake Michigan. *J. Appl. Meteor.*, **17**, 1843–1855, [https://doi.org/10.1175/1520-0450\(1978\)017<1843:LBCOTW>2.0.CO;2](https://doi.org/10.1175/1520-0450(1978)017<1843:LBCOTW>2.0.CO;2).
- Kilpatrick, K. A., and Coauthors, 2015: A decade of sea surface temperature from MODIS. *Remote Sens. Environ.*, **165**, 27–41, <https://doi.org/10.1016/j.rse.2015.04.023>.
- Knievel, J. C., D. L. Rife, J. A. Grim, A. N. Hahmann, J. P. Hacker, M. Ge, and H. H. Fisher, 2010: A simple technique for creating regional composites of sea surface temperature from MODIS for use in operational mesoscale NWP. *J. Appl. Meteor. Climatol.*, **49**, 2267–2284, <https://doi.org/10.1175/2010JAMC2430.1>.
- LADCO, 1995: Executive summary. Lake Michigan Ozone Control Program Project Rep., Vol. I, Lake Michigan Ozone Study, Lake Michigan Air Directors Consortium.
- Lee, P., F. Ngan, H. Lei, B. Baker, B. Dornblaser, G. McGahey, and D. Tong, 2014: An application for improving air quality (a Houston case study). *Earthzine*, <https://earthzine.org/2014/03/29/an-application-for-improving-air-quality-a-houston-case-study/>.
- , and Coauthors, 2017: NAQFC developmental forecast guidance for fine particulate matter (PM_{2.5}). *Wea. Forecasting*, **32**, 343–360, <https://doi.org/10.1175/WAF-D-15-0163.1>.
- Levy, I., and Coauthors, 2010: Unraveling the complex local-scale flows influencing ozone patterns in the southern Great Lakes of North America. *Atmos. Chem. Phys.*, **10**, 10 895–10 915, <https://doi.org/10.5194/acp-10-10895-2010>.
- Loughner, C. P., and Coauthors, 2014: Impact of bay-breeze circulations on surface air quality and boundary layer export. *J. Appl. Meteor. Climatol.*, **53**, 1697–1713, <https://doi.org/10.1175/JAMC-D-13-0323.1>.
- Louis, J. F., 1979: A parametric model of vertical eddy fluxes in the atmosphere. *Bound.-Layer Meteor.*, **17**, 187–202, <https://doi.org/10.1007/BF00117978>.
- Lyons, W. A., and H. S. Cole, 1976: Photochemical oxidant transport: Mesoscale lake breeze and synoptic-scale aspects. *J. Appl. Meteor.*, **15**, 733–743, [https://doi.org/10.1175/1520-0450\(1976\)015<0733:POTMLB>2.0.CO;2](https://doi.org/10.1175/1520-0450(1976)015<0733:POTMLB>2.0.CO;2).
- Ma, L.-M., and Z.-M. Tan, 2009: Improving the behavior of the cumulus parameterization for tropical cyclone prediction: Convective trigger. *Atmos. Res.*, **92**, 190–211, <https://doi.org/10.1016/j.atmosres.2008.09.022>.
- Mackaro, S., R. T. McNider, and A. Pour-Biazar, 2011: Some physical and computational issues in land surface data assimilation of satellite skin temperatures. *Pure Appl. Geophys.*, **169**, 401–414, <https://doi.org/10.1007/s00024-011-0377-0>.
- McNider, R. T., and R. A. Pielke, 1981: Diurnal boundary-layer development over sloping terrain. *J. Atmos. Sci.*, **38**, 2198–2212, [https://doi.org/10.1175/1520-0469\(1981\)038<2198:DBLDOS>2.0.CO;2](https://doi.org/10.1175/1520-0469(1981)038<2198:DBLDOS>2.0.CO;2).
- , A. J. Song, D. M. Casey, P. J. Wetzel, W. L. Crosson, and R. M. Rabin, 1994: Toward a dynamic–thermodynamic assimilation of satellite surface temperature in numerical atmospheric models. *Mon. Wea. Rev.*, **122**, 2784–2803, [https://doi.org/10.1175/1520-0493\(1994\)122<2784:TADTAO>2.0.CO;2](https://doi.org/10.1175/1520-0493(1994)122<2784:TADTAO>2.0.CO;2).
- , J. A. Song, and S. Q. Kidder, 1995: Assimilation of GOES-derived solar insolation into a mesoscale model for studies of cloud shading effects. *Int. J. Remote Sens.*, **16**, 2207–2231, <https://doi.org/10.1080/01431169508954552>.
- , W. B. Norris, D. M. Casey, J. E. Pleim, S. J. Roselle, and W. M. Lapenta, 1998: Assimilation of satellite data in regional air quality models. *Air Pollution Modeling and Its Application XII*, S. E. Gryning and N. Chaumerliac, Eds., NATO Challenges of Modern Society Series, Vol. 22, 25–35.
- , W. M. Lapenta, A. P. Biazar, G. J. Jedlovec, R. J. Suggs, and J. Pleim, 2005: Retrieval of model grid-scale heat capacity using geostationary satellite products. Part I: First case-study application. *J. Appl. Meteor.*, **44**, 1346–1360, <https://doi.org/10.1175/JAM2270.1>.
- , and Coauthors, 2012: Response and sensitivity of the nocturnal boundary layer over land to added longwave radiative forcing. *J. Geophys. Res.*, **117**, D14106, <https://doi.org/10.1029/2012JD017578>.
- , K. Doty, Y. L. Wu, and A. Pour Biazar, 2017: Use of satellite data to improve specifications of land surface parameters. AORP Project 16-039 Final Rep., 119 pp., http://aqrp.ceer.utexas.edu/projectinfoFY16_17/17-039/17-039%20Final%20Report.pdf.
- Mellor, G. L., and T. Yamada, 1982: Development of a turbulence closure model for geophysical fluid problems. *Rev. Geophys.*, **20**, 851–875, <https://doi.org/10.1029/RG020i004p00851>.
- Morrison, H., and A. Gettelman, 2008: A new two-moment bulk stratiform cloud microphysics scheme in the Community Atmosphere Model, version 3 (CAM3). Part I: Description and numerical tests. *J. Climate*, **21**, 3642–3659, <https://doi.org/10.1175/2008JCLI2105.1>.
- , G. Thompson, and V. Tatarskii, 2009: Impact of cloud microphysics on the development of trailing stratiform precipitation in a simulated squall line: Comparison of one- and two-moment schemes. *Mon. Wea. Rev.*, **139**, 1013–1035, <https://doi.org/10.1175/2008MWR2556.1>.
- Ngan, F., H. Kim, P. Lee, K. Al-Wali, and B. Dornblaser, 2013: A study of nocturnal surface wind speed overprediction by the WRF-ARW model in southeastern Texas. *J. Appl. Meteor. Climatol.*, **52**, 2638–2653, <https://doi.org/10.1175/JAMC-D-13-060.1>.
- Niu, G. Y., and Coauthors, 2011: The community Noah land surface model with multiparameterization options (Noah-MP): 1. Model description and evaluation with local-scale measurements. *J. Geophys. Res.*, **116**, D12109, <https://doi.org/10.1029/2010JD015139>.
- Noilhan, J., and S. Planton, 1989: A simple parameterization of land surface processes for meteorological models. *Mon. Wea. Rev.*, **117**, 536–549, [https://doi.org/10.1175/1520-0493\(1989\)117<0536:ASPOLS>2.0.CO;2](https://doi.org/10.1175/1520-0493(1989)117<0536:ASPOLS>2.0.CO;2).
- Pierce, B., R. Kaleel, A. Dickens, T. Bertram, C. Stanier, and D. Kenski, 2017: White Paper: Lake Michigan Ozone Study 2017 (LMOS 2017). LADCO, 22 pp., http://www.ladco.org/reports/ozone/post08/Great_Lakes_Ozone_Study_White_Paper_Draft_v6.pdf.
- Pitman, A. J., 2003: The evolution of, and revolution in, land surface schemes designed for climate models. *Int. J. Climatol.*, **23**, 479–510, <https://doi.org/10.1002/joc.893>.

- Pleim, J. E., 2006: A simple, efficient solution of flux–profile relationships in the atmospheric surface layer. *J. Appl. Meteor. Climatol.*, **45**, 341–347, <https://doi.org/10.1175/JAM2339.1>.
- , 2007: A combined local and nonlocal closure model for the atmospheric boundary layer. Part II: Application and evaluation in a mesoscale meteorological model. *J. Appl. Meteor. Climatol.*, **46**, 1396–1409, <https://doi.org/10.1175/JAM2534.1>.
- , and A. Xiu, 1995: Development and testing of a surface flux and planetary boundary layer model for application in mesoscale models. *J. Appl. Meteor.*, **34**, 16–32, [https://doi.org/10.1175/1520-0450\(1995\)34<16:DOALSM>2.0.CO;2](https://doi.org/10.1175/1520-0450(1995)34<16:DOALSM>2.0.CO;2).
- , and —, 2003: Development of a land surface model. Part II: Data assimilation. *J. Appl. Meteor.*, **42**, 1811–1812, [https://doi.org/10.1175/1520-0450\(2003\)042<1811:DOALSM>2.0.CO;2](https://doi.org/10.1175/1520-0450(2003)042<1811:DOALSM>2.0.CO;2).
- , and R. Gilliam, 2009: An indirect data assimilation scheme for deep soil temperature in the Pleim–Xiu land surface model. *J. Appl. Meteor. Climatol.*, **48**, 1362–1376, <https://doi.org/10.1175/2009JAMC2053.1>.
- , A. Xiu, P. L. Finkelstein, and T. L. Otte, 2001: A coupled land-surface and dry deposition model and comparison to field measurements of surface heat, moisture, and ozone fluxes. *Water Air Soil Pollut. Focus*, **1**, 243–252, <https://doi.org/10.1023/A:1013123725860>.
- Poulos, G. S., and Coauthors, 2002: CASES-99: A comprehensive investigation of the stable nocturnal boundary layer. *Bull. Amer. Meteor. Soc.*, **83**, 555–581, [https://doi.org/10.1175/1520-0477\(2002\)083<0555:CACIOT>2.3.CO;2](https://doi.org/10.1175/1520-0477(2002)083<0555:CACIOT>2.3.CO;2).
- Pour-Biazar, A., and Coauthors, 2007: Correcting photolysis rates on the basis of satellite observed clouds. *J. Geophys. Res.*, **112**, D10302, <https://doi.org/10.1029/2006JD007422>.
- Ran, L., J. Pleim, R. Gilliam, F. S. Binkowski, C. Hogrefe, and L. Band, 2016: Improved meteorology from an updated WRF/CMAQ modeling system with MODIS vegetation and albedo. *J. Geophys. Res. Atmos.*, **121**, 2393–2415, <https://doi.org/10.1002/2015JD024406>.
- Rosero, E., Z.-L. Yang, L. E. Gulden, G.-Y. Niu, and D. J. Gochis, 2009: Evaluating enhanced hydrological representations in Noah-LSM over transition zones: Implications for model development. *J. Hydrometeorol.*, **10**, 600–662, <https://doi.org/10.1175/2009JHM1029.1>.
- Savijärvi, H., 2009: Stable boundary layer: Parametrizations for local and larger scales. *Quart. J. Roy. Meteor. Soc.*, **135**, 914–921, <https://doi.org/10.1002/qj.423>.
- Sellers, P. J., and Coauthors, 1997: Modeling the exchanges of energy, water, and carbon between continents and the atmosphere. *Science*, **275**, 502–509, <https://doi.org/10.1126/science.275.5299.502>.
- Sillman, S., 1995: New developments in understanding the relation between ozone, NO_x and hydrocarbons in urban atmospheres. *Progress and Problems in Atmospheric Chemistry*, J. R. Barker, Ed., Advanced Series in Physical Chemistry, Vol. 3, World Scientific, 145–171, https://doi.org/10.1142/9789812831712_0005.
- Siuta, D., G. West, and R. Stull, 2017: WRF hub-height wind forecast sensitivity to PBL scheme, grid length, and initial condition choice in complex terrain. *Wea. Forecasting*, **32**, 493–509, <https://doi.org/10.1175/WAF-D-16-0120.1>.
- Skamarock, W. C., and Coauthors, 2008: A description of the Advanced Research WRF version 3. NCAR Tech. Note NCAR/TN-475+STR, 113 pp., <https://doi.org/10.5065/D68S4MVH>.
- Steenefeld, G. J., T. Mauritsen, E. I. F. De Bruijn, J. Vilà-Guerau de Arellano, G. Svensson, and A. A. M. Holtslag, 2008: Evaluation of limited-area models for the representation of the diurnal cycle and contrasting nights in CASES-99. *J. Appl. Meteor. Climatol.*, **47**, 869–887, <https://doi.org/10.1175/2007JAMC1702.1>.
- Sun, J., and L. Mahrt, 1995: Determination of surface fluxes from the surface radiative temperature. *J. Atmos. Sci.*, **52**, 1096–1106, [https://doi.org/10.1175/1520-0469\(1995\)052<1096:DOSFFT>2.0.CO;2](https://doi.org/10.1175/1520-0469(1995)052<1096:DOSFFT>2.0.CO;2).
- Thiébaux, J., E. Rogers, W. Wang, and B. Katz, 2003: A new high-resolution blended global sea surface temperature analysis. *Bull. Amer. Meteor. Soc.*, **84**, 645–656, <https://doi.org/10.1175/BAMS-84-5-645>.
- Ukkola, A. M., M. G. De Kauwe, A. J. Pitman, M. J. Best, G. Abramowitz, V. Haverd, M. Decker, and N. Haughton, 2016: Land surface models systematically overestimate the intensity, duration and magnitude of seasonal-scale evaporative droughts. *Environ. Res. Lett.*, **11**, 104012, <https://doi.org/10.1088/1748-9326/11/10/104012>.
- Wagener, T., and H. V. Gupta, 2005: Model identification for hydrological forecasting under uncertainty. *Stochastic Environ. Res. Risk Assess.*, **19**, 378–387, <https://doi.org/10.1007/s00477-005-0006-5>.
- Wetzel, P. J., D. Atlas, and R. H. Woodward, 1984: Determining soil moisture from geosynchronous satellite infrared data: A feasibility study. *J. Climate Appl. Meteor.*, **23**, 375–391, [https://doi.org/10.1175/1520-0450\(1984\)023<0375:DSMFGS>2.0.CO;2](https://doi.org/10.1175/1520-0450(1984)023<0375:DSMFGS>2.0.CO;2).
- White, A. T., A. Pour-Biazar, K. Doty, B. Dornblaser, and R. T. McNider, 2018: Improving cloud simulation for air quality studies through assimilation of geostationary satellite observations in retrospective meteorological modeling. *Mon. Wea. Rev.*, **146**, 29–48, <https://doi.org/10.1175/MWR-D-17-0139.1>.
- Yang, R., and M. A. Friedl, 2003: Modeling the effects of three-dimensional vegetation structure on surface radiation and energy balance in boreal forests. *J. Geophys. Res.*, **108**, 8615, <https://doi.org/10.1029/2002JD003109>.